

INFORMATION TO USERS

The most advanced technology has been used to photograph and reproduce this manuscript from the microfilm master. UMI films the text directly from the original or copy submitted. Thus, some thesis and dissertation copies are in typewriter face, while others may be from any type of computer printer.

The quality of this reproduction is dependent upon the quality of the copy submitted. Broken or indistinct print, colored or poor quality illustrations and photographs, print bleedthrough, substandard margins, and improper alignment can adversely affect reproduction.

In the unlikely event that the author did not send UMI a complete manuscript and there are missing pages, these will be noted. Also, if unauthorized copyright material had to be removed, a note will indicate the deletion.

Oversize materials (e.g., maps, drawings, charts) are reproduced by sectioning the original, beginning at the upper left-hand corner and continuing from left to right in equal sections with small overlaps. Each original is also photographed in one exposure and is included in reduced form at the back of the book.

Photographs included in the original manuscript have been reproduced xerographically in this copy. Higher quality 6" x 9" black and white photographic prints are available for any photographs or illustrations appearing in this copy for an additional charge. Contact UMI directly to order.

U·M·I

University Microfilms International
A Bell & Howell Information Company
300 North Zeeb Road, Ann Arbor, MI 48106-1346 USA
313/761-4700 800/521-0600

Order Number 9020767

Theory of the inhomogeneous electron gas

Harbola, Manoj Kumar, Ph.D.

City University of New York, 1990

U·M·I
300 N. Zeeb Rd.
Ann Arbor, MI 48106

A

THEORY OF THE INHOMOGENEOUS ELECTRON GAS

by

MANOJ K. HARBOLA

A dissertation submitted to the Graduate Faculty in
Physics in partial fulfillment of the requirements
for the degree of Doctor of Philosophy, The City
University of New York.

1990

This manuscript has been read and accepted for the Graduate Faculty in Physics in satisfaction of the dissertation requirements for the degree of Doctor of Philosophy.

Nov. 28, 1989.

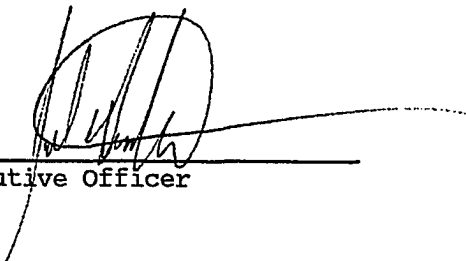
Date

Vincent A. S. S.

Chairman of Examining Committee

Nov 28 1989

Date


Executive Officer

V. Sahni
J.B. Krieger
P.A. Montano
J.I. Gersten
M.W. Cole

Supervisory Committee

The City University of New York

Abstract

THEORY OF THE INHOMOGENEOUS ELECTRON GAS

by

Manoj K. Harbola

Adviser: Prof. Virahat Sahni

In this thesis we present a physical interpretation for the local many-body (exchange-correlation) potential of Hohenberg-Kohn-Sham density-functional theory of the interacting inhomogeneous electron gas. Thus far this potential has been known only in terms of its mathematical definition as the functional derivative of the yet unknown exchange-correlation energy functional. We interpret the potential as the work done in moving an electron in the electric field produced by its Fermi-Coulomb hole charge distribution. Thus, with this interpretation this potential is obtained directly from the Fermi-Coulomb hole, the requirement of determining the functional derivatives being obviated. Within the exchange-only approximation, the potential derived by our interpretation is shown analytically to satisfy the virial theorem sum rule for the exact exchange energy functional, a necessary condition for the exchange potentials of density-functional theory, as well as all scaling properties of such potentials. A significant consequence of the interpretation is that the asymptotic structure of the exchange-correlation potential is shown to be due to Pauli correlation effects alone, and therefore can be determined exactly. The interpretation also provides the

explanation as to why the Slater potential is incorrect. The formalism is applied to closed subshell atoms and jellium metal surfaces within the exchange-only approximation. The self-consistently determined total ground-state energies of atoms are rigorous upper bounds to and lie within 50 ppm of the results of Hartree-Fock theory. Furthermore, since the exchange potential is the exact exchange-correlation potential in the outer and asymptotic regions of the atom, the highest occupied eigenvalues more closely approximate the experimental ionization potential, and asymptotically the potential goes as $-(1/r)$. For jellium metal surfaces it is shown that for asymptotic positions of the electron the exchange potential goes as the image potential $-(1/4x)$. Inside the metal, the exchange potential is lowered to a value of $-2/3$ (in units of $3k_F/2\pi$), the exact homogeneous electron gas result of Kohn-Sham theory.

ACKNOWLEDGEMENTS

This work has been done under the able guidance of Professor Viraht Sahni. I wish to express my gratitude for the time and effort he has devoted in teaching and training me. His enthusiasm has been a constant source of inspiration for me. I would also like to thank Professor Sahni for the encouragement and support he has always provided during my stay at Brooklyn college.

I would also like to express my thanks to the other members of the committee, Professor J.B. Kriger and Profesor P.A. Montano of Brooklyn College, Professor J.I. Gersten of The City College and Professor M.W. Cole of Pennsylvania State University, for their helpful advice.

Special thanks to Professor Krieger of Brooklyn College for his stimulating discussions. I would also like to thank Professor Krieger and Dr. Li for collaboration on the atomic self-consistent calculations.

CONTENTS

Abstract.	.iii
List of Tables.	viii
List of Figures.	.iv
Chapter I: INTRODUCTION.	.1
Chapter II: QUANTUM-MECHANICAL INTERPRETATION OF THE EXCHANGE-CORRELATION POTENTIAL OF KOHN-SHAM DENSITY-FUNCTIONAL THEORY.	17
2.1 The Physical Interpretation.	17
2.2 Discussion of Slater Theory and Other Approximation Schemes.	25
2.3 The W_x Potential for the Argon Atom: A Non ^x Self-Consistent Application.	30
Chapter III: APPLICATION TO THE INHOMOGENEOUS ELECTRON GAS AT METALLIC SURFACES.	35
3.1 Structure of the Fermi Hole at Metallic Surfaces.	.39
3.2 Structure of the Slater Potential at Metallic Surfaces.	.47
3.3 Structure of the Potential W_x at Metallic Surfaces.	.52
Chapter IV: GROUND-STATE ENERGIES AND HIGHEST OCCUPIED EIGENVALUES OF ATOMS IN EXCHANGE-ONLY APPROXIMATION (SELF-CONSISTENT APPLICATION).	63
4.1 Ground-State Energies.	64
4.2 Highest Occupied Eigenenergies.	.66
4.3 Comparison with the Optimized Potential Method Results.	.66
Chapter V: CONCLUSION.	74
Appendix A: EXPRESSION FOR THE FERMI HOLE AND THE CORRESPONDING ELECTRIC FIELD FOR CLOSED SUBSHELL ATOMS.	82

Appendix B: FERMİ HOLE AT METALLIC SURFACES. 85

**Appendix C: ASYMOTOTIC BEHAVIOR OF THE PLANAR
AVERAGED FERMİ HOLE AT METALLIC SURFACES. 87**

**Appendix D: EXACT SLATER POTENTIAL AT
METALLIC SURFACES. 91**

**Appendix E: THE ELECTRIC FIELD ϵ_x AND THE POTENTIAL
 W_x DUE TO THE FERMİ HOLE AT
METALLIC SURFACES. 93**

REFERENCES. 95

LIST OF TABLES

Table I: Work W_x (in units of $3k_F/2\pi$) done against the electric field of the Fermi hole of an electron as it is removed from inside the metal to asymptotic distances outside the metal surface. 60

Table II: Ground State atomic energies in the Pauli-correlated approximation. 65

Table III: Highest occupied eigenvalues of atoms in the Pauli-correlated approximation. 67

Table IV: Comparison of the exchange energies $E_x[\Psi_i]$ in atomic units as determined from the orbitals Ψ_i with those obtained from the potential W_x as given by the expression on the right hand side of the virial theorem sum rule [Eq. (1.32)]. 72

LIST OF FIGURES

- Figure 1:** Variation of W_x , the Optimized Potential Method (OPM), and the Slater potentials for the Argon atom.31
- Figure 2:** Variation of the cross section of the Fermi hole $\rho_x(\mathbf{r}, \mathbf{r}')$ in the plane of electron removal perpendicular to the surface versus $y' = k_F x'$ for different positions y of the electron in the vacuum region. [Eq. (3.6)].42
- Figure 3:** Variation of the radial distribution of the Fermi hole charge density in planes at y' parallel to the surface versus the distance from the axis of electron removal [Eq. (3.4)] for different positions y of the electron outside the surface. The solid lines correspond to the quantum-mechanical charge distribution and the dashed lines represent the classical distribution of charge. [Eq. (3.8)].44
- Figure 4:** Variation of the total exchange charge between $-y$ and ∞ as given by the integral $-\int_{-y}^{\infty} \rho_x(y, y') dy'$ versus the electron position y46

Figure 5: Variation of the universal function $v_x^{Sl}(y)/(3k_F/2\pi)$, where $v_x^{Sl}(y)$ is the Slater potential [Eq. (3.11)], versus the electron position y . The function $1/y$ and the image potential $(\pi/6)/y$ are also plotted. 49

Figure 6: Variation of the universal function $v_x^{Sl}(y)/(3k_F/2\pi)$, where $v_x^{Sl}(y)$ is the Slater potential [Eq. (3.11)], for asymptotic positions y of the electron outside the surface. The function $1/y$ and the image potential $(\pi/6)/y$ are also plotted. 51

Figure 7: Variation of the universal function $\epsilon_x(y)/(3k_F^2/2\pi)$, where $\epsilon_x(y)$ is the electric field due to the Fermi hole [Eq. (3.13)], versus the electron position y 54

Figure 8: Variation of the universal function $\epsilon_x(y)/(3k_F^2/2\pi)$, where $\epsilon_x(y)$ is the electric field due to the Fermi hole [Eq. (3.13)], for asymptotic positions y of the electron outside the surface. The function $1/y^2$ is also plotted. 55

Figure 9: Variation of the universal function $W_x(y)/(3k_F/2\pi)$, where $W_x(y)$ is the work done against the electric field $\epsilon_x(y')$ due to the Fermi hole [Eq. (3.14)], versus the electron position y . The function $-1/2y$ is also plotted. 57

Figure 10: The self-consistently determined W_x and the Optimized Potential Method (OPM) potentials for the Xenon atom in the interior of the atom. 69

Figure 11: The self-consistently determined W_x and the Optimized Potential Method (OPM) potentials for the Xenon atom in the region exterior to the shells. 70

Chapter I

INTRODUCTION

The solution of the Schrodinger equation provides the basis for determining the properties of the interacting electronic systems in atoms, molecules, and solids. However, for a system of N electrons, the Schrodinger equation is a $3N$ dimensional differential equation and our ability to find exact solutions is rather limited. The problem can thus be solved only in an approximate manner. The application of the variational principle for the energy in conjunction with approximate wavefunctions has given rise to methods such as the Hartree¹, Hartree-Fock,² configuration-interaction,³ and correlated wavefunction⁴ techniques. The principle attribute of these methods is that they lead to rigorous upper bounds for the ground-state energy, but they are in general difficult to apply to systems involving more than a few electrons. The complexity lies in the fact that one still has to solve for the wavefunction $\Psi(\mathbf{r}_1, \mathbf{r}_2, \dots, \mathbf{r}_N)$ which involves $3N$ variables. Thus, for example, although solutions for atoms in the Hartree-Fock approximation exist,² the self-consistent solution of these equations for the many-electron non-uniform system at metallic surfaces has yet to be achieved.⁵

Attempts to avoid solving the complicated Schrodinger equation have given rise to statistical methods such as the Thomas-Fermi⁶ method and its extensions.⁶ The basic idea in these theories is that the energy may be expressed in terms of the electronic density $\rho(\mathbf{r})$, a

function of only three variables which is defined as:

$$\rho(\mathbf{r}) = \sum_i^N \int |\Psi(\mathbf{r}_1, \dots, \mathbf{r}_i = \mathbf{r}, \dots, \mathbf{r}_N)|^2 d\mathbf{r}_1 d\mathbf{r}_2 \dots d\mathbf{r}_{i-1} d\mathbf{r}_{i+1} \dots d\mathbf{r}_N . \quad (1.1)$$

Although these statistical methods are simpler to apply, they do not lead to rigorous bounds for the energy since they treat the many-body effects and their dependence on the density in an approximate manner. Hohenberg and Kohn,⁷ however, have proved rigorously that in fact there is a one-to-one correspondence between the exact ground-state multiparticle wavefunction $\Psi(\mathbf{r}_1, \mathbf{r}_2, \dots, \mathbf{r}_N)$ that has all the many-body effects in it and the density $\rho(\mathbf{r})$ of the system. Thus, the expectation values of all the observables including the ground-state energy, can be expressed as functionals of the density.

The ground-state energy⁸ of a many-electron system is a functional of the ground-state wavefunction $\Psi(\mathbf{r}_1, \mathbf{r}_2, \dots, \mathbf{r}_N)$ and is given as:

$$E[\Psi] = T + V + U \quad (1.2)$$

where T is the kinetic energy

$$T = \frac{1}{2} \sum_i^N \int \nabla_i \Psi^*(\mathbf{r}_1, \mathbf{r}_2, \dots, \mathbf{r}_i, \dots, \mathbf{r}_N) \cdot \nabla_i \Psi(\mathbf{r}_1, \mathbf{r}_2, \dots, \mathbf{r}_i, \dots, \mathbf{r}_N) d\mathbf{r}_1 d\mathbf{r}_2 \dots d\mathbf{r}_i \dots d\mathbf{r}_N , \quad (1.3)$$

V the external potential energy

$$V = \sum_i^N \int \Psi^*(\mathbf{r}_1, \mathbf{r}_2, \dots, \mathbf{r}_i, \dots, \mathbf{r}_N) v(\mathbf{r}_i) \Psi(\mathbf{r}_1, \mathbf{r}_2, \dots, \mathbf{r}_i, \dots, \mathbf{r}_N) d\mathbf{r}_1 d\mathbf{r}_2 \dots d\mathbf{r}_i \dots d\mathbf{r}_N, \quad (1.4)$$

and U the electron-electron interaction energy

$$U = \frac{1}{2} \sum_{i \neq j} \int \frac{1}{|\mathbf{r}_i - \mathbf{r}_j|} \Psi^*(\mathbf{r}_1, \mathbf{r}_2, \dots, \mathbf{r}_i, \dots, \mathbf{r}_j, \dots, \mathbf{r}_N) \Psi(\mathbf{r}_1, \mathbf{r}_2, \dots, \mathbf{r}_i, \dots, \mathbf{r}_j, \dots, \mathbf{r}_N) d\mathbf{r}_1 d\mathbf{r}_2 \dots d\mathbf{r}_i \dots d\mathbf{r}_j \dots d\mathbf{r}_N. \quad (1.5)$$

Now according to the Hohenberg-Kohn theorem,⁷ there is a one-to-one relationship between the external potential $v(\mathbf{r})$ and the ground-state density $\rho(\mathbf{r})$. It follows that since $v(\mathbf{r})$ determines $\Psi(\mathbf{r}_1, \mathbf{r}_2, \dots, \mathbf{r}_N)$ uniquely via the Schrodinger equation, so will the density $\rho(\mathbf{r})$. Thus the energy functional in Eq. (1.2) can alternatively be written as a functional $E[\rho]$ of the density $\rho(\mathbf{r})$. Further, since the functional $E[\rho]$ has the lowest value for the correct Ψ , so will be the case for $E[\rho]$ for the correct ground-state density. Thus the Rayleigh-Ritz variational principle can also be applied to the functional $E[\rho]$ with respect to the density. The minimization of the energy then gives rise to the Euler equation for the density

$$\frac{\delta E[\rho]}{\delta \rho(\mathbf{r})} - \mu = 0, \quad (1.6)$$

where μ is the Lagrange multiplier which ensures the conservation of the number of particles:

$$N = \int \rho(\mathbf{r}) \, d\mathbf{r} . \quad (1.7)$$

Thus, in principle it is possible to obtain the exact ground-state density $\rho(\mathbf{r})$ and energy E for a system of N interacting particles by solving the Euler equation. This approach is also much simpler than the application of the Rayleigh-Ritz variational principle to the functional $E[\Psi]$ because the minimization with respect to Ψ involves $3N$ variables, whereas the minimization of $E[\rho]$ is with respect to $\rho(\mathbf{r})$, a function of only three variables. In practice, however, it is not possible to obtain the exact solution of Eq. (1.6) as the functional $E[\rho]$ is not known exactly. The Thomas-Fermi method and its extensions are approximations⁷ to the exact Euler equation.

An alternate approach to solving Eq. (1.6) that treats the kinetic and electrostatic energies exactly is provided by the Kohn-Sham⁹ (KS) version of density-functional theory. In this scheme the energy functional $E[\rho]$ is written as a sum of a kinetic energy functional $E_k[\rho]$ of a system of non-interacting electrons having the same density distribution as for the interacting system, the Hartree electrostatic energy $E_{es}[\rho]$, and an "exchange-correlation" energy functional $E_{xc}[\rho]$. By splitting the energy functional in this way, all the many-body effects are incorporated in the exchange-correlation energy functional $E_{xc}[\rho]$. Thus, in density-functional theory, the exchange and correlation energy values differ¹⁰ from those of

conventional quantum mechanics. Now Eq. (1.6) for the density can be shown⁹ to be equivalent to solving the set of single particle Kohn-Sham equations

$$\left\{ -\frac{1}{2} \nabla^2 + v_{\text{eff}}^{\text{KS}}[\rho(\mathbf{r}); \mathbf{r}] \right\} \varphi_i(\mathbf{r}) = \varepsilon_i \varphi_i(\mathbf{r}) , \quad (1.8)$$

where $v_{\text{eff}}^{\text{KS}}[\rho(\mathbf{r}); \mathbf{r}]$ is the local (multiplicative) effective potential in which all the electrons move. The orbitals $\varphi_i(\mathbf{r})$ of the Kohn-Sham equations lead to the ground-state density via

$$\rho(\mathbf{r}) = \sum_i |\varphi_i(\mathbf{r})|^2 , \quad (1.9)$$

and thereby to the ground-state energy. These orbitals, however, have no physical significance in themselves and cannot be interpreted as electronic wavefunctions because although the Kohn-Sham equation has the same form as the Schrodinger equation, the two are not the same.

The Kohn-Sham effective potential $v_{\text{eff}}^{\text{KS}}[\rho(\mathbf{r}); \mathbf{r}]$ is the sum of the Hartree electrostatic $V_{\text{es}}(\mathbf{r})$ and exchange-correlation $\mu_{\text{xc}}(\mathbf{r})$ potentials:

$$v_{\text{eff}}^{\text{KS}}[\rho(\mathbf{r}); \mathbf{r}] = V_{\text{es}}(\mathbf{r}) + \mu_{\text{xc}}(\mathbf{r}) , \quad (1.10)$$

where as a consequence of the variational principle for the energy,

these potentials are derived⁹ to be the functional derivatives

$$V_{\text{es}}(\mathbf{r}) = \frac{\delta E_{\text{es}}[\rho]}{\delta \rho(\mathbf{r})} \quad (1.11)$$

and

$$\mu_{\text{xc}}(\mathbf{r}) = \frac{\delta E_{\text{xc}}[\rho]}{\delta \rho(\mathbf{r})} \quad (1.12)$$

respectively. If the external potential is assumed to be due to a charge distribution $\rho_+(\mathbf{r})$, such that the total charge $\rho_t(\mathbf{r})$ distribution is

$$\rho_t(\mathbf{r}) = \rho_+(\mathbf{r}) + \rho(\mathbf{r}) , \quad (1.13)$$

then the electrostatic energy is

$$E_{\text{es}}[\rho] = \frac{1}{2} \iint \frac{\rho_t(\mathbf{r})\rho_t(\mathbf{r}')}{|\mathbf{r}-\mathbf{r}'|} \, d\mathbf{r}d\mathbf{r}' , \quad (1.14)$$

and the corresponding potential $V_{\text{es}}(\mathbf{r})$ via Eq. (1.11) is

$$V_{\text{es}}(\mathbf{r}) = v(\mathbf{r}) + \int \frac{\rho(\mathbf{r}')}{|\mathbf{r}-\mathbf{r}'|} \, d\mathbf{r}' . \quad (1.15)$$

The exchange-correlation energy functional $E_{xc}[\rho]$ is defined as

$$E_{xc}[\rho] = \int \epsilon_{xc}(\mathbf{r}) \rho(\mathbf{r}) d\mathbf{r} , \quad (1.16)$$

where $\epsilon_{xc}(\mathbf{r})$ is the exchange-correlation energy per particle. On a more fundamental level, the exchange-correlation energy in density-functional theory¹⁰ may be thought¹¹⁻¹³ of as the Coulomb interaction energy between the electronic density and the Fermi-Coulomb (hole) charge density $\rho_{xc}(\mathbf{r}, \mathbf{r}')$ at \mathbf{r}' for an electron at \mathbf{r} . The hole is a consequence of the reduction in probability of electrons approaching each other due to the Pauli exclusion principle and the Coulomb repulsion between electrons. Thus we may write

$$E_{xc}[\rho] = \frac{1}{2} \iint \frac{\rho(\mathbf{r}) \rho_{xc}(\mathbf{r}, \mathbf{r}')}{|\mathbf{r} - \mathbf{r}'|} d\mathbf{r} d\mathbf{r}' , \quad (1.17)$$

where the Fermi-Coulomb hole charge density is given as

$$\rho_{xc}(\mathbf{r}, \mathbf{r}') = \rho(\mathbf{r}') \int_0^1 d\lambda [g_\lambda(\mathbf{r}, \mathbf{r}') - 1] , \quad (1.18)$$

and where $g_\lambda(\mathbf{r}, \mathbf{r}')$ is the pair correlation function of the system with density $\rho(\mathbf{r})$ and coupling constant λ . The Fermi-Coulomb hole is comprised of a positive charge equal in magnitude to that of an electron and thus satisfies the charge neutrality sum rule

$$\int \rho_{xc}(\mathbf{r}, \mathbf{r}') d\mathbf{r}' = 1 . \quad (1.19)$$

Now since all the many-body effects are embodied in $E_{xc}[\rho]$, it is clear from the above interpretation of $E_{xc}[\rho]$ that in density functional theory¹⁰ it is the Fermi-Coulomb hole that accounts for all the complexities of the many-electron problem.

In exchange-only density-functional theory,^{10,14} in which only correlations between electrons due to the Pauli exclusion principle are considered in the construction of the wavefunction, the fundamental property of interest is the Fermi hole charge distribution $\rho_x(\mathbf{r}, \mathbf{r}')$. The reduction in probability of electrons approaching each other due to the Pauli exclusion principle is given by the expression

$$\rho_x(\mathbf{r}, \mathbf{r}') = |\gamma(\mathbf{r}, \mathbf{r}')|^2 / 2\rho(\mathbf{r}) , \quad (1.20)$$

where $\gamma(\mathbf{r}, \mathbf{r}')$ is the single-particle density matrix defined as

$$\gamma(\mathbf{r}, \mathbf{r}') = \sum_i \psi_i^*(\mathbf{r}') \psi_i(\mathbf{r}) \quad (1.21)$$

and which satisfies the condition

$$\gamma^*(\mathbf{r}, \mathbf{r}') = \gamma(\mathbf{r}', \mathbf{r}) . \quad (1.22)$$

In addition to satisfying the charge conservation sum rule

$$\int \rho_x(\mathbf{r}, \mathbf{r}') \, d\mathbf{r}' = 1 , \quad (1.23)$$

the Fermi hole also satisfies the conditions

$$\rho_{\mathbf{x}}(\mathbf{r}, \mathbf{r}) = \rho(\mathbf{r})/2 , \quad (1.24)$$

and

$$\rho_{\mathbf{x}}(\mathbf{r}, \mathbf{r}') \geq 0 . \quad (1.25)$$

The lowering of the energy due to Pauli correlations, viz. the exchange energy $E_{\mathbf{x}}[\rho]$, may also be interpreted as the interaction energy between an electron and its Fermi hole charge and therefore written as

$$E_{\mathbf{x}}[\rho] = \frac{1}{2} \iint \frac{\rho(\mathbf{r}) \rho_{\mathbf{x}}(\mathbf{r}, \mathbf{r}')}{|\mathbf{r} - \mathbf{r}'|} d\mathbf{r} d\mathbf{r}' . \quad (1.26)$$

The corresponding Kohn-Sham exchange potential $\mu_{\mathbf{x}}(\mathbf{r})$ is then the functional derivative

$$\mu_{\mathbf{x}}(\mathbf{r}) = \frac{\delta E_{\mathbf{x}}[\rho]}{\delta \rho(\mathbf{r})} , \quad (1.27)$$

and the exchange-only^{10,14} Kohn-Sham equations which define the orbitals $\psi_i(\mathbf{r})$ to be employed in the construction of the Fermi hole are

$$\left[-\frac{1}{2} \nabla^2 + V_{\text{es}}(\mathbf{r}) + \mu_{\mathbf{x}}(\mathbf{r}) \right] \psi_i(\mathbf{r}) = \epsilon_i \psi_i(\mathbf{r}) . \quad (1.28)$$

The Slater determinant of the orbitals $\psi_i(\mathbf{r})$ simultaneously¹⁰ minimizes the expectation value of the Hamiltonian. However, since the $\psi_i(\mathbf{r})$

are also eigenfunctions of a local potential, the total ground-state energies in exchange-only density-functional theory must lie above those of Hartree-Fock theory. For the homogeneous electron gas the potential μ_x (in units of $3k_F/2\pi$, where k_F is the Fermi momentum) has⁷ the exact value of $-(2/3)$.

Now in the fully-correlated case, the exchange-correlation energy functional $E_{xc}[\rho]$ may be written as a sum of its exchange $E_x[\rho]$ and correlation $E_c[\rho]$ energy components. As a consequence, the Fermi-Coulomb hole $\rho_{xc}(\mathbf{r},\mathbf{r}')$ may be thought of as being comprised of its Fermi $\rho_x(\mathbf{r},\mathbf{r}')$ and Coulomb $\rho_c(\mathbf{r},\mathbf{r}')$ hole charge distributions so that

$$\rho_{xc}(\mathbf{r},\mathbf{r}') = \rho_x(\mathbf{r},\mathbf{r}') + \rho_c(\mathbf{r},\mathbf{r}') . \quad (1.29)$$

The orbitals to be employed¹⁰ in the construction of these holes are those of the Kohn-Sham equation [Eq. 1.8] with the full exchange-correlation potential. Since both the Fermi-Coulomb and Fermi holes satisfy the same charge conservation sum rule [see Eqs.(1.19) and (1.23)], it follows (with these definitions of the Fermi and Coulomb holes) that

$$\int \rho_c(\mathbf{r},\mathbf{r}') d\mathbf{r}' = 0 , \quad (1.30)$$

or that the total Coulomb hole charge is zero. The correlation energy $E_c[\rho]$ is then the interaction energy between an electron and its Coulomb hole and the correlation potential μ_c is the functional

derivative

$$\mu_c(\mathbf{r}) = \frac{\delta E_c[\rho]}{\delta \rho(\mathbf{r})} . \quad (1.31)$$

With the exception of the highest occupied eigenvalue ϵ_{\max} , the eigenenergies of the Kohn-Sham equations [Eq. (1.8)] are not physical removal energies.¹⁵ The eigenvalue ϵ_{\max} , however, has been shown^{16,17} to be the negative of the ionization energy or chemical potential. It has also been shown¹⁸⁻²⁰ by examples that the exact Kohn-Sham Fermi surface is generally not the same as the physical one.

Since in Kohn-Sham theory the kinetic energy is that of a system of non-interacting electrons, the difference T_c between the interacting and non-interacting system kinetic energies is absorbed in the exchange-correlation energy functional $E_{xc}[\rho]$. When this functional is further divided into its exchange $E_x[\rho]$ and correlation $E_c[\rho]$ components, the difference in the kinetic energies T_c is entirely absorbed into the correlation energy functional. In density-functional theory, therefore, there are no exchange contributions T_x to the kinetic energy: the kinetic and exchange energies are in this sense independent of each other. This is also the case in exchange-only density functional theory. With these definitions and the application of the virial theorem, it has been shown²¹ that for arbitrary density $\rho(\mathbf{r})$, the exchange and correlation energy

functionals and their functional derivatives satisfy the sum rules

$$\begin{aligned}
 -E_x[\rho] &\equiv \frac{1}{2} \sum_{i,j} \iint \frac{\varphi_i^*(\mathbf{r}) \varphi_j^*(\mathbf{r}') \varphi_i(\mathbf{r}') \varphi_j(\mathbf{r})}{|\mathbf{r}-\mathbf{r}'|} d\mathbf{r}d\mathbf{r}' \\
 &\quad (\text{|| spins}) \\
 &= \int d\mathbf{r} \rho(\mathbf{r}) \mathbf{r} \cdot \nabla \mu_x(\mathbf{r}) , \quad (1.32)
 \end{aligned}$$

and

$$E_c[\rho] + \int d\mathbf{r} \rho(\mathbf{r}) \mathbf{r} \cdot \nabla \mu_c(\mathbf{r}) = -T_c[\rho] < 0 . \quad (1.33)$$

With the above density-functional theory definitions, it can also readily be seen²¹ that the kinetic and exchange energies, and the exchange potential scale as $E_k[\rho_\lambda] = \lambda^2 E_k[\rho]$, $E_x[\rho_\lambda] = \lambda E_x[\rho]$ and $\mu_x(\rho_\lambda) = \lambda \mu_x(\rho)$ respectively, where $\varphi_{i,\lambda}(\mathbf{r}) = \lambda^{3/2} \varphi_i(\lambda \mathbf{r})$ so that $\rho_\lambda(\mathbf{r}) = \lambda^3 \rho(\lambda \mathbf{r})$. These scaling laws do not apply to the interacting kinetic energy nor to the exchange energy of Hartree-Fock theory.

The solution of the Kohn-Sham equations (Eq. 1.8) lead in principle to the ground-state density, total ground-state energy, and to the non-relativistic ionization potential of interacting electronic systems in the presence of an external potential. However, neither the exchange-correlation $E_{xc}[\rho]$, nor the exchange $E_x[\rho]$ or the correlation $E_c[\rho]$ energy functionals of the density are known explicitly. The exchange energy functional $E_x[\rho]$ is, however, known in terms of the Kohn-Sham orbitals. As a consequence, the functional derivatives of these functionals which constitute part of the local Kohn-Sham effective potential are all unknown. In terms of the Fermi-Coulomb

$\rho_{xc}(\mathbf{r}, \mathbf{r}')$ and Fermi $\rho_x(\mathbf{r}, \mathbf{r}')$ hole charge distributions, this means that the functional dependence of these quantities on the density $\rho(\mathbf{r})$ is also unknown.

Thus, although Hohenberg-Kohn-Sham theory makes the profound advance of reducing the complexity of the many-electron problem, the exact Kohn-Sham equation cannot be explicitly written. This is the case even in the exchange-only approximation of density-functional theory. (In contrast, the Hartree-Fock equations, though more complex due to the presence of the non-local exchange operator, are precisely known). It is the reduction in mathematical complexity that has, however, inspired the search for the unknown energy functionals in terms of the density. Thus, since its inception, a principal thrust^{15,22-25} of research in density-functional theory has been towards the development of accurate exchange-correlation energy functionals, particularly in forms for which the functional derivatives could easily be obtained. The best known and most widely used of these approximations is the local density approximation^{9,26}. In this approximation each point of the inhomogeneous electron gas is treated as if it were homogeneous but with the local value of the density. However, once the exchange-correlation or correlation energy functionals are approximated, the rigor of the Hohenberg-Kohn theorem is lost, and as a consequence the bounds for the total energy are no longer rigorous. Furthermore, the accuracy of an energy functional by no means guarantees the accuracy of its functional derivative. Thus, even if one employs an accurate approximation to the exchange-correlation energy functional, the solutions of the Kohn-Sham

equations may not be as accurate because it is the functional derivative that appears in these equations.

In this thesis we provide²⁷ a physical interpretation for the exchange-correlation, (and exchange and correlation) potentials of Kohn-Sham density-functional theory. With this interpretation these potentials may be determined directly from the Fermi and Coulomb hole charge distributions of the electron, as is the case for the corresponding energies. Thus the potential is obtained purely on the basis of physical considerations without any recourse to the variational principle for the energy. The lack of explicit application of the variational principle obviates the need to determine functional derivatives.

In Chapter II section 2.1 we present the physical arguments leading to the construction of the exchange-correlation potential of Kohn-Sham theory. The implications of this interpretation with regard to the structure of the potential are also discussed. We then prove that in the exchange-only theory, the potential thus constructed satisfies the virial theorem sum rule of Eq. (1.32) exactly. In section 2.2 we discuss and compare our interpretation in the exchange-only approximation with Slater²⁸ theory and the Optimized Potential Method²⁹⁻³¹. We also discuss approximation schemes for fully-correlated systems, such as the X α method of Slater et al,³² the Kohn-Sham local density approximation^{7,9} for exchange and correlation as well as the Hartree-Fock-Slater approximation²⁸ for exchange, and the gradient expansion approximation,^{7,9} in terms of the

interpretation presented. In section 2.3 we apply our formalism to obtain the exchange potential for the Argon atom in a non-self-consistent manner, and compare our results with those of the Optimized Potential Method as obtained by Talman and co-workers^{30,31} and with the Slater potential.

To demonstrate the universality of our interpretation we apply our formalism in Chapter III in a non-self-consistent application to the many-electron inhomogeneous gas at metallic surfaces.³³ The calculations are performed within the exchange-only approximation, and as such we begin in section 3.1 with a study³⁴ of the three dimensional structure of the Fermi hole at a metal surface. In this section we extend the work of Sahni and Bohnen³⁵ to asymptotic positions of the electron outside the surface. We show rigorously³⁴ that the Fermi hole charge is not localized to the surface region but rather spread throughout the semi-infinite crystal by proving that its center of mass is singular. We also compare the quantum-mechanical and classical charge distributions for these asymptotic electron positions. In section 3.2 we determine^{36,37} the structure of the Slater potential at metal surfaces, and compare it with the image potential for asymptotic positions of the electron from the surface. Finally, in section 3.3 we obtain³⁸ the exchange potential at a metal surface as determined via our interpretation of the local effective potential.

In Chapter IV we apply³⁹ our formalism to obtain fully-self-consistent results for the total ground-state energies and highest occupied eigenvalues of closed subshell atoms within the

exchange-only approximation. Comparisons of the resulting total energies are then made with those of Hartree-Fock theory², and of the highest occupied eigenvalues with experimental⁴⁰ ionization potentials. Comparisons of the local exchange potential are also made with the Talman et al^{30,31} optimized potentials.

Finally, in our concluding Chapter V we evaluate our formalism in the context of density-functional theory both from a strictly theoretical viewpoint as well as by the results of application. We also discuss directions for future research.

Chapter II

**QUANTUM-MECHANICAL INTERPRETATION OF THE EXCHANGE-CORRELATION
POTENTIAL OF KOHN-SHAM DENSITY-FUNCTIONAL THEORY**

2.1 The Physical Interpretation

In order to understand the physical interpretation of the exchange-correlation potential of Kohn-Sham theory, let us recall the physical meaning of the electrostatic energy $E_{es}[\rho]$ and potential $V_{es}(\mathbf{r})$. The electrostatic energy is the energy of interaction between the electrons and the total charge distribution $\rho_t(\mathbf{r})$, which is a static distribution of charge. (The expression Eq. (1.14) includes the Coulomb self-energy of the external charge). The potential $V_{es}(\mathbf{r})$, as given by Eq. (1.15) is the potential energy of an electron in the presence of this static charge distribution. Thus, it is the work done in bringing an electron from the reference point at infinity to its final position at \mathbf{r} against the electric field $\epsilon_{es}(\mathbf{r})$ due to this charge distribution. The potential so obtained is well defined because the field is conservative: its curl vanishes and therefore the work done is path independent. From a strictly mathematical viewpoint, the electrostatic potential V_{es} is the functional derivative [Eq. (1.11)] of the electrostatic energy functional $E_{es}[\rho]$.

Now since the exchange-correlation energy $E_{xc}[\rho]$ may be thought of as the interaction energy between the electronic density $\rho(\mathbf{r})$ and the Fermi-Coulomb hole charge distribution $\rho_{xc}(\mathbf{r}, \mathbf{r}')$, the corresponding exchange-correlation potential of an electron may be interpreted²⁷ as the work $W_{xc}(\mathbf{r})$ done to bring it from infinity against the electric

field $\epsilon_{xc}(\mathbf{r})$ of the Fermi-Coulomb hole distribution. However, in contrast to the electronic and external charge distributions which are static, the Fermi-Coulomb hole is a dynamic^{34,35,41} (non-local) charge distribution: the structure of this distribution depends explicitly on the electron position. As such the exchange-correlation potential cannot be written in a manner similar to that of the electrostatic potential as

$$\int \frac{\rho_{xc}(\mathbf{r}, \mathbf{r}')}{|\mathbf{r} - \mathbf{r}'|} d\mathbf{r}' . \quad (2.1)$$

To account for the dynamic nature of the Fermi-Coulomb charge in determining the potential it gives rise to, the electric field $\epsilon_{xc}(\mathbf{r})$ due to this charge, which according to Coulomb's law is given as

$$\epsilon_{xc}(\mathbf{r}) = \int \frac{\rho_{xc}(\mathbf{r}, \mathbf{r}') (\mathbf{r} - \mathbf{r}')}{|\mathbf{r} - \mathbf{r}'|^3} d\mathbf{r}' , \quad (2.2)$$

must first be determined. The potential is then obtained by calculating the work done in moving the electron in this field. Thus, the local effective exchange-correlation $W_{xc}(\mathbf{r})$ potential seen by the electrons is given by the line integral

$$W_{xc}(\mathbf{r}) = - \int_{\infty}^{\mathbf{r}} \epsilon_{xc}(\mathbf{r}') \cdot d\mathbf{l}' . \quad (2.3)$$

With this interpretation for the exchange-correlation potential, the differential equation to be solved for the determination of the properties of an interacting electronic system is

$$\left[-\frac{1}{2} \nabla^2 + V_{es}(\mathbf{r}) + W_{xc}(\mathbf{r}) \right] \Psi_i(\mathbf{r}) = \epsilon_i \Psi_i(\mathbf{r}) \quad (2.4a)$$

or

$$\left[-\frac{1}{2} \nabla^2 + V_{es}(\mathbf{r}) + W_x(\mathbf{r}) + W_c(\mathbf{r}) \right] \Psi_i(\mathbf{r}) = \epsilon_i \Psi_i(\mathbf{r}) \quad (2.4b)$$

where the electronic density is

$$\rho(\mathbf{r}) = \sum_i |\Psi_i(\mathbf{r})|^2 \quad (2.5)$$

In Eq. (2.4b), the exchange, W_x and correlation, W_c potentials are the work done against the electric fields ϵ_x and ϵ_c due to the Fermi $\rho_x(\mathbf{r}, \mathbf{r}')$ and the Coulomb $\rho_c(\mathbf{r}, \mathbf{r}')$ hole charges respectively. In the exchange-only approximation, the hole due to Coulomb correlations is ignored, and thus in this approximation Eq. (2.4b) is solved with $W_c = 0$. Observe that in contrast to the Kohn-Sham equations in which the exchange-correlation potential is obtained as the functional derivative of an energy functional, in the present formalism, these potentials are determined directly from the Fermi-Coulomb (or Fermi or Coulomb) hole charge distributions. Thus, with the above physical interpretation, the local exchange-correlation potential of Kohn-Sham theory can be obtained without having to determine the functional derivatives.

In the exchange-only theory, whereas the exact Kohn-Sham potential μ_x is unknown, the potential $W_x(\mathbf{r})$ is known precisely since the Fermi hole can be constructed explicitly in terms of the orbitals of Eq. (2.4b) with $W_c = 0$. Furthermore, since the potential $W_x(\mathbf{r})$ is local, the complexity of solution of the differential equation in this approximation should be far less than that of solving the Hartree-Fock equations. The resulting W_x -formalism total ground-state energies will, however, be rigorous upper bounds to the Hartree-Fock energy. Thus, whereas in Kohn-Sham theory both the exchange and correlation potentials must be approximated, only the Coulomb hole and therefore the correlation potential need be approximated in the present formalism.

With the interpretation that the exchange-correlation potential is the work done in moving the electron in the electric field of the non-local Fermi-Coulomb hole charge distribution, the question arises as to whether the potential so obtained is path independent. Equivalently, does the curl of the electric field $\epsilon_{xc}(\mathbf{r})$ vanish? For symmetric systems such as spherically symmetric atoms and jellium metal surfaces this certainly is the case. For surfaces the electric field is in the direction perpendicular to the surface and a function only of the co-ordinate in this direction, making the curl vanish. For spherically symmetric densities, the field is in the radial direction and a function of only the radial co-ordinate, and therefore in this case too the curl of the field vanishes. For systems of arbitrary symmetry, the curl of the electric field as defined above may not be zero. However, as will be shown by application in this

thesis, the concept of obtaining the potential from the electric field arising from the Fermi-Coulomb hole charge distribution is fundamental to the interacting electron gas problem. Thus, for systems for which the curl of the field is not zero, the exchange-correlation potential can be constructed from the longitudinal component $\epsilon_{xc,l}(\mathbf{r})$ of the electric field, thus ensuring the path independence of the potential. This component of the field is given by the expression

$$\epsilon_{xc,l}(\mathbf{r}) = -\frac{1}{4\pi} \nabla \int \frac{\mathbf{v}' \cdot \epsilon_{xc}(\mathbf{r}')}{|\mathbf{r}-\mathbf{r}'|} d\mathbf{r}' . \quad (2.6)$$

For symmetric systems, the electric field and its longitudinal component are equivalent.

In Kohn-Sham theory the local many-body potential $\mu_{xc}(\mathbf{r})$ is defined strictly mathematically as the functional derivative of the exchange-correlation energy functional. The question which we next address is whether the potential $W_{xc}(\mathbf{r})$ as given by the above interpretation is equivalent to the one obtained by taking the functional derivative? Let us first consider this question in the exchange-only approximation. The exchange energy functional $E_x[\rho]$ and its functional derivative $\mu_x(\mathbf{r})$ satisfy the virial theorem sum rule of Eq. (1.32). This is a necessary condition that the local exchange potential must satisfy. Replacing $\mu_x(\mathbf{r})$ in Eq. (1.32) by $W_x(\mathbf{r})$, and noting that

$$-\nabla W_x(\mathbf{r}) = \epsilon_x(\mathbf{r}) \quad (2.7)$$

for systems for which the curl of the electric field is zero, we have on substituting for $\epsilon_{\mathbf{x}}(\mathbf{r})$ from Eq. (2.2) and $\rho_{\mathbf{x}}(\mathbf{r},\mathbf{r}')$ from Eq. (1.20) that

$$\begin{aligned} E_{\mathbf{x}}[\rho] &= \iint \rho(\mathbf{r}) \rho_{\mathbf{x}}(\mathbf{r},\mathbf{r}') \frac{\mathbf{r} \cdot (\mathbf{r}-\mathbf{r}')}{|\mathbf{r}-\mathbf{r}'|^3} d\mathbf{r}d\mathbf{r}' \\ &= \frac{1}{2} \iint |\gamma(\mathbf{r},\mathbf{r}')|^2 \frac{\mathbf{r} \cdot (\mathbf{r}-\mathbf{r}')}{|\mathbf{r}-\mathbf{r}'|^3} d\mathbf{r}d\mathbf{r}' . \end{aligned} \quad (2.8)$$

Since

$$|\gamma(\mathbf{r},\mathbf{r}')|^2 = |\gamma(\mathbf{r}',\mathbf{r})|^2 , \quad (2.9)$$

Eq. (2.8) may be rewritten by interchanging \mathbf{r} and \mathbf{r}' as

$$E_{\mathbf{x}}[\rho] = -\frac{1}{2} \iint |\gamma(\mathbf{r},\mathbf{r}')|^2 \frac{\mathbf{r}' \cdot (\mathbf{r}-\mathbf{r}')}{|\mathbf{r}-\mathbf{r}'|^3} d\mathbf{r}d\mathbf{r}' . \quad (2.10)$$

Adding Eqs. (2.8) and (2.9) and dividing by 2 gives

$$E_{\mathbf{x}}[\rho] = \frac{1}{4} \iint \frac{|\gamma(\mathbf{r},\mathbf{r}')|^2}{|\mathbf{r}-\mathbf{r}'|^3} d\mathbf{r}d\mathbf{r}' , \quad (2.11)$$

which is Eq. (1.26) as written in terms of the single particle density matrix. Thus the work $W_{\mathbf{x}}$ satisfies the necessary condition for it to be the functional derivative of $E_{\mathbf{x}}[\rho]$. This, ofcourse, does not prove that $W_{\mathbf{x}}$ is the Kohn-Sham potential since there may exist several functions which when added to $W_{\mathbf{x}}$ will give a vanishing contribution to the right hand side of the sum rule of Eq. (1.32). However, although such functions may exist, what their origin from a fundamental physical viewpoint would be is unclear. In this context we note that the

Pauli exclusion principle has already been accounted for in the construction of the Fermi hole, and in exchange-only theory it is only this quantum-mechanical effect that has to be invoked. Furthermore, the local exchange potential W_x scales as

$$W_x(\rho_\lambda) = \lambda W_x(\rho) \quad (2.12)$$

which indicates that it falls within the rubric of density-functional theory exchange potentials. We are unaware at present of any physically derivable exchange potentials which satisfy both the virial theorem sum rule as well as the scaling law.

In the virial theorem sum rule for Coulomb correlations Eq. (1.33), which relates the correlation energy $E_c[\rho]$ to its functional derivative μ_c , the difference T_c between the kinetic energies of the interacting and non-interacting systems also appears in the expression. Its contribution $\delta T_c / \delta \rho$ to the potential is non-electromagnetic in nature, and may therefore not be accounted for by this interpretation which is based on Coulomb's law. Consequently, such a term may have to be added to W_c to obtain the true Kohn-Sham correlation (or exchange-correlation) potential. We expect this contribution to be small in comparison to the full exchange plus correlation potentials. For atoms and molecules, T_c is typically of the same order of magnitude as the correlation energy.

An important consequence of the physical interpretation given to the exchange-correlation potential W_{xc} is that its structure for

asymptotic positions of the electron is known exactly and is that of the exchange potential W_x alone. This is so because the total Coulomb hole charge is zero [Eq. (1.30)] and therefore does not contribute to the work W_c for these electron positions. The potential W_c is nonzero only in those regions for which the electron is within or about the Coulomb hole charge distribution. Thus, by solving the many electron problem in the exchange-only approximation, the correct asymptotic structure of the potential for the fully-correlated system is automatically determined.

To solve for the fully-correlated interacting electron gas systems within the present formalism, approximate forms of the Coulomb or the Fermi-Coulomb hole, such as those within the random phase approximation, must be employed. The more accurate the representation of the Coulomb hole the more accurate will be the results for the ground-state energy, ionization potential and other properties. However, approximating the Coulomb hole charge density implies that the bounds for the ground-state energy are no longer rigorous.

Finally, we observe that since the W_{xc} equation (2.4) has not been derived by application of the variational principle for the energy, it may also be solved for excited states of the interacting system. Since the Fermi-Coulomb charge distributions for electrons in their ground and excited states are different, so will be the corresponding potentials these charges give rise to. However, we would like to point out here that although the Hohenberg-Kohn-Sham theory guarantees the existence of a local effective potential for electrons

in the ground state, there is no mathematical proof that such a local potential exists for the excited states also. Our proposition that excited states can also be described by a local potential is based on the fact that the physical arguments that are given for the construction of the local potential for the ground-state are equally applicable for the excited states.

2.2 Discussion of Slater Theory and Other Approximation Schemes

We begin this section with a discussion of the physical basis of the Slater²⁸ theory. In this theory too, the non-local exchange operator of Hartree-Fock theory is replaced by a local multiplicative potential. However the arguments²⁸ leading to the construction of this potential are not mathematically rigorous, and therefore the Slater theory is an approximate scheme for solving the many-electron problem in the exchange-only approximation. In Hartree-Fock theory according to Slater²⁸, each electron can be thought of as moving in an orbital-dependent exchange potential $V_{x,i}$ given as

$$V_{x,i}(\mathbf{r}) = \int \frac{\rho_{x,i}(\mathbf{r},\mathbf{r}')}{|\mathbf{r}-\mathbf{r}'|} d\mathbf{r}' , \quad (2.13)$$

which is produced by the orbital-dependent exchange charge density or Fermi hole $\rho_{x,i}(\mathbf{r},\mathbf{r}')$. For an electron in the i th state, the orbital dependent exchange-charge at \mathbf{r}' for an electron at \mathbf{r} is defined as

$$\rho_{x,i}(\mathbf{r},\mathbf{r}') = \frac{\sum_j \psi_j^*(\mathbf{r}') \psi_j(\mathbf{r}) \psi_i(\mathbf{r}')}{\psi_i(\mathbf{r})} , \quad (2.14)$$

where the orbitals $\psi_i(\mathbf{r})$ are the solutions of the Hartree-Fock equations. Due to the orthonormality of the wavefunctions, the orbital-dependent Fermi hole satisfies the charge conservation sum rule

$$\int \rho_{\mathbf{x},i}(\mathbf{r},\mathbf{r}') d\mathbf{r}' = 1 . \quad (2.15)$$

Furthermore, at the position of the electron its value is

$$\rho_{\mathbf{x},i}(\mathbf{r},\mathbf{r}'=\mathbf{r}) = \rho(\mathbf{r})/2 , \quad (2.16)$$

where $\rho(\mathbf{r})$ is the density of electrons at \mathbf{r} . Thus, the orbital-dependent exchange-charge density satisfies the same sum rules as those satisfied by the Fermi hole [Eqs. (1.23) and (1.24)] discussed in Chapter I. However, as opposed to the Fermi hole which is always positive [see Eq. (1.25)], the orbital-dependent charge can have negative values^{37,41}. Now Slater²⁸ argued that the orbital-dependent charge densities could not be very different from each other since each satisfied the sum rules given by Eqs. (2.15) and (2.16). He therefore assumed that no great error would be made if instead one employed a weighted mean of these orbital-dependent densities, weighted by the probability of occupation of each state. Thus, according to Slater the average Fermi hole is given as

$$\begin{aligned} \rho_{\mathbf{x}}^{\text{Sl}}(\mathbf{r},\mathbf{r}') &= \frac{\sum_i \rho_{\mathbf{x},i}(\mathbf{r},\mathbf{r}') \psi_i^*(\mathbf{r}) \psi_i(\mathbf{r})}{\sum_i \psi_i^*(\mathbf{r}) \psi_i(\mathbf{r})} \\ &= \frac{\sum_{i,j} \psi_i^*(\mathbf{r}) \psi_j^*(\mathbf{r}') \psi_i(\mathbf{r}') \psi_j(\mathbf{r})}{\sum_i \psi_i^*(\mathbf{r}) \psi_i(\mathbf{r})} . \end{aligned} \quad (2.17)$$

Note that the Slater averaged hole is the same as the Fermi hole $\rho_x(\mathbf{r}, \mathbf{r}')$ given in Chapter I [Eq. (1.20)] which gives the reduction in probability of electrons approaching each other due to the Pauli exclusion principle. This charge distribution, ofcourse, is orbital independent. On the basis of this distribution of charge, the local potential proposed ad hoc by Slater to approximate the orbital dependent potential $V_{x,i}$ of Hartree-Fock theory was

$$V_x^{Sl}(\mathbf{r}) = \int \frac{\rho_x(\mathbf{r}, \mathbf{r}')}{|\mathbf{r} - \mathbf{r}'|} d\mathbf{r}' . \quad (2.18)$$

Although the potential above appears to have been derived on the basis of reasonable approximations, the physics behind the derivation is incorrect. The Fermi hole is a dynamic^{34,35,41} charge distribution so that it changes as a function of electron position. However the Slater potential is calculated as if the Fermi hole were static. Thus the Slater potential would be exact only if the Fermi hole were a local rather than a non-local charge distribution. The incorrectness of this potential is evident⁹ even in the simplest case of the homogeneous electron gas for which its value (in units of $3k_F/2\pi$) is -1 instead of the correct Kohn-Sham result of $-(2/3)$. From a mathematical viewpoint the Slater potential is incorrect because it is not the functional derivative of the exchange energy functional as written in terms of the Fermi hole charge distribution $\rho_x(\mathbf{r}, \mathbf{r}')$ [see Eq. (1.26)]. Nonetheless, it is interesting to note that although the orbital-dependent Fermi hole charge distributions (for each electron position) are significantly different^{37,42}, the expression for the

Fermi hole obtained by Slater's averaging process is correct. Slater's error lay in the way he treated this charge distribution in order to determine the corresponding potential.

Slater²⁸ further approximated the potential proposed by him by treating it within the local density approximation (LDA). Thus the Hartree-Fock-Slater potential, as it is known, is given as

$$V_x^{\text{Sl,LDA}}(\mathbf{r}) = \frac{3k_F(\mathbf{r})}{2\pi} \quad , \quad (2.19)$$

where $k_F(\mathbf{r}) = [3\pi^2\rho(\mathbf{r})]^{1/3}$ is the local value of the Fermi momentum. The local density approximation corresponds to replacing the pair-correlation function of the interacting electron gas by the homogeneous electron gas result. Thus the expression Eq.(1.18) for the Fermi-Coulomb hole charge density is replaced in the local density approximation by

$$\rho_{\text{xc}}^{\text{LDA}}(\mathbf{r},\mathbf{r}') = \rho(\mathbf{r}) \int_0^1 d\lambda [g_\lambda^{\text{hom}}\{|\mathbf{r}-\mathbf{r}'|;\rho(\mathbf{r})\} - 1] \quad , \quad (2.20)$$

where g_λ^{hom} is the pair-correlation function for the homogeneous electron gas of density $\rho(\mathbf{r})$. Since in this approximation the density $\rho(\mathbf{r})$ is assumed to be uniform for each electron position \mathbf{r} , the corresponding Fermi-Coulomb hole is spherically symmetric about the electron and satisfies the charge conservation sum rule of Eq. (1.19). In the exchange-only case, the pair-correlation function for the uniform electron gas is known exactly,⁴³ and thus so is the local density approximation Fermi hole. However, with the interpretation

for the local exchange-correlation potential given in the previous section, it is clear that in the local density approximation the work done vanishes for all electron positions. This is so because the spherically symmetric Fermi-Coulomb hole gives zero electric field at the electron. The Hartree-Fock-Slater²⁸ approximation is, therefore, wrong on two counts: one, it treats the Fermi hole as if it were static, and two, it assumes that the hole follows the electron in a manner such that its structure is always spherically symmetric about it. It is for the latter reason that the local density approximation of Kohn-Sham theory for exchange and correlation is also based on a weak physical foundation. The $X\alpha$ method of Slater et al³² for taking Coulomb correlation effects into account is also a local density scheme. In this method the potential of Eq. (2.19) is multiplied by a parameter α , and the total energy minimized with respect to this parameter. Therefore, this scheme too is fundamentally in error from a physical viewpoint. Thus the local density approximation, though exact for the uniform electron gas, is weakly founded for nonuniform systems.

In the ad hoc gradient expansion approximation,^{7,9} valid for slowly varying densities, the Fermi-Coulomb hole is more realistic⁴⁴ in that in regions of high density it is no longer centered about the electron. The corresponding potential obtained from this charge distribution is therefore more accurate in regions which contribute most to the energy. In regions where the density is very slowly varying, the gradient expansion approximation hole approaches⁴⁴ that of the local density approximation, and therefore the highest occupied

eigenvalues as obtained within these approximations are similar and significantly in error.

Before proceeding to the next section where we present quantitative results, we describe here briefly the optimized-potential-method²⁹⁻³¹ (OPM) which can in principle give the exact Kohn-Sham potential in the exchange-only approximation.^{10,14} The OPM is a purely mathematical scheme that determines variationally a central potential which minimizes the expectation value of the Hartree-Fock Hamiltonian. The result of the variation is a complex linear integral equation for the local exchange potential. Since the orbitals in this scheme are obtained from a local potential, the ground-state energies obtained by this method are rigorous upper bounds to the Hartree-Fock energy. However, as in the case of Hartree-Fock theory for finite systems, the highest occupied eigenvalue of the OPM can not be interpreted as the negative of the ionization potential. The OPM equation has been solved for atoms by Talman and co-workers^{30,31}. Thus, it is meaningful to compare the potential W_x for atoms with the OPM potential as obtained by Talman et al.³¹

2.3 The W_x Potential for the Argon Atom (a non self-consistent application)

In this section we present the interpretations, ideas, and explanations of the previous two sections in quantitative terms. We calculate the potential W_x for the Argon atom employing the orbitals generated by Talman et al.³¹. (The use of analytical Hartree-Fock wavefunctions⁴⁵ leads to essentially the same results). In Fig. 1 we

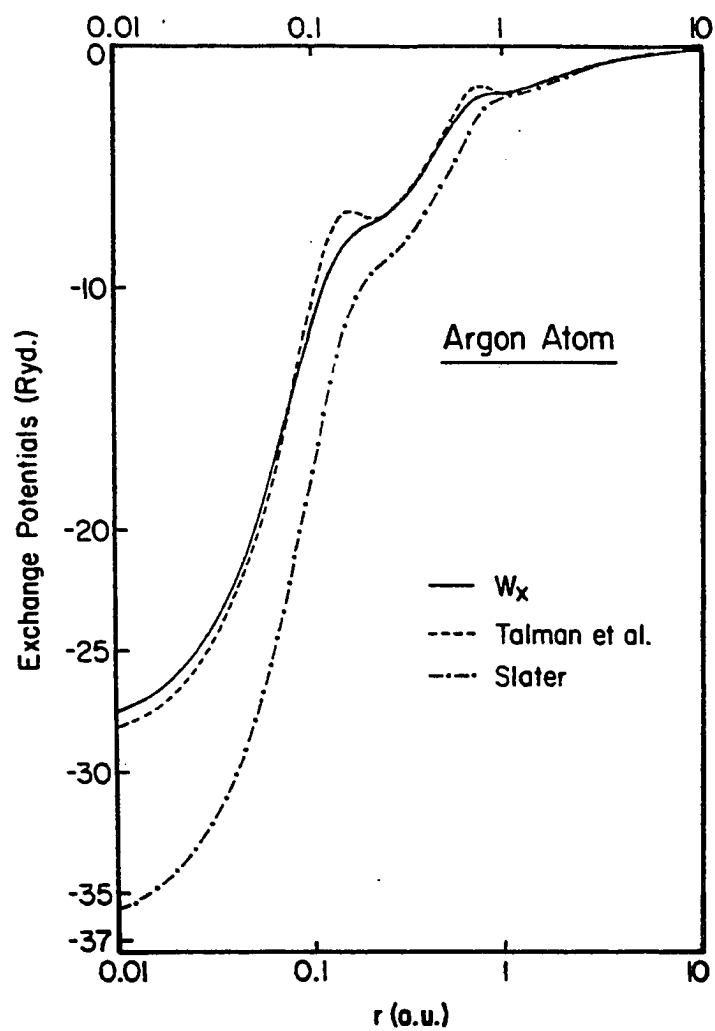


FIG. 1. Variation of W_x , the Optimized Potential Method (OPM), and the Slater potentials for the Argon atom.

plot the exchange potential W_x as determined²⁷ by our interpretation of it as being the work done against the electric field of the Fermi-Coulomb hole charge distribution. The expression for the Fermi hole and the corresponding electric field are given in Appendix A. We observe that the function W_x is monotonic with positive slope everywhere. This implies that the work done in removing the electron is always positive. The potential displays a distinct change in slope as the electron moves through the intershell regions, thereby clearly delineating the shell structure of the atom. Asymptotically the potential goes as $-(1/r)$ as it must. That the potential W_x must be $-(1/r)$ is also clear from a physical viewpoint because the Fermi hole has a total charge of unity localized about the center of the atom. The result thus is in agreement with our statement that the asymptotic structure of the potential for fully-correlated systems is that of W_x alone. The result is also consistent with detailed derivations^{46,47} for atoms which show that $\mu_{xc} \sim -(1/r) - (\alpha/2r^4)$ as $r \rightarrow \infty$, where α is the polarizability of the positive ion, and where the leading term is due to exchange effects alone.

The exchange potential of Talman et al³¹ is also plotted in Fig. 1. A study of the W_x and Talman potentials shows that in the deep interior of the atom upto and including the K shell, which is the region from which the principal contribution⁴³ to the energy arises, the two curves are essentially equivalent. They are also indistinguishable in the L and M shell regions. The value of the Talman and W_x potentials at the nucleus, for example, are -28.1297 Ry. and -27.3940 Ry. respectively. Asymptotically the Talman potential also

falls off as $-(1/r)$. Talman and Shadwick³⁰ have proved mathematically that the linear integral equations of the OPM do lead to this structure. It is only in the intershell regions that the Talman and W_x curves differ, the former exhibiting bumps. These bumps have been given no physical interpretation thus far. The bumps too delineate the shell structure of the atom. For completeness, we would like to point out here that although the OPM potentials should in principle satisfy the virial theorem based sum rule of Eq. (1.32), the actual calculations - due to their numerical complexity - lead to potentials that do not satisfy it to a high degree of accuracy. When the Talman orbitals are substituted into Eq. (1.32), the left and right hand sides of the sum rule differ, and are -60.32 Ry. and -59.94 Ry. respectively. On the other hand, substitution of the work W_x as calculated by the Talman orbitals into the sum rule leads to a value of -60.32 Ry as it must. Further discussion on the comparison of the potentials is relegated to Chapter IV where the potential W_x is determined fully self-consistently.

The Slater potential of Eq. (2.18) is also plotted in Fig. 1. The Slater potential significantly overestimates both the W_x and the Talman potentials over the entire atom. At the nucleus the Slater potential value is -35.6533 Ry. The Slater potential too does not possess any bumps in the intershell region. Asymptotically, the Slater potential does go correctly as $-(1/r)$. This is due to the fact that for electron positions far from the nucleus, the Fermi hole stabilizes⁴⁸ and is localized about the nucleus with its center of mass being at it. Thus, this static charge gives a potential which goes as

$-(1/r)$. The only reason why the Slater potential has the correct asymptotic behaviour is that for these electron positions the Fermi hole is no longer dynamic. Thus we see that a potential constructed by not taking into account the dynamic nature of the Fermi hole is significantly in error.

Chapter III

APPLICATION TO THE INHOMOGENEOUS ELECTRON GAS AT METALLIC SURFACES

In order to demonstrate the universality of our interpretation of the local exchange-correlation potential, we apply it in this chapter to the inhomogeneous electron gas at metallic surfaces³³. As opposed to the few-electron atomic system problem, this is a many-electron nonuniform system that is in addition extended. Since the expression for the Fermi hole charge distribution is known explicitly, we again perform our calculations within the exchange-only approximation. As such we begin in section 3.1 by a discussion and study³⁴ of the three-dimensional structure of the Fermi hole at metallic surfaces. This is an extension of the work of Sahni and Bohnen³⁵ to asymptotic positions of the electron outside the metal. In addition we show³⁴ that the Fermi hole charge is spread throughout the semi-infinite crystal and that its center of mass is singular. Comparisons of this quantum-mechanical charge with the classical image charge for these asymptotic positions of the electron are also made.

In section 3.2 we demonstrate the consequences of treating the dynamical Fermi hole charge as if it were static by calculating^{36,37} the Slater potential. We show that asymptotically far from the metal surface the Slater potential approaches a value of $-(1/2x)$, where x is the distance of the electron from the surface, which is twice the image potential. In the interior of the metal the Slater potential goes to the erroneous Slater homogeneous electron gas result^{27,37,38} of -1 (in units of $3k_F/2\pi$). We note that if the classical image

charge were treated as a static charge distribution, the corresponding potential outside the surface is also $-(1/2x)$, and not the image potential. Thus both the quantum-mechanical and the classical potentials are the same if the charge distributions from which they are derived are considered to be static. This fact demonstrates the consistency, albeit for an erroneous result, between the quantum-mechanical and classical pictures for electrons that are far outside the metal surface. It also demonstrates that electrons asymptotically far from the surface can in fact be considered as distinguishable particles.

Finally in section 3.3 we explicitly consider the non-local nature of the Fermi hole and determine³⁸ the work W_x done against the electric field of this charge distribution. We show that for asymptotic positions of the electron far from the metal surface, the potential goes as $-(1/4x)$, the image potential. As discussed in section 2.1, this is also the asymptotic structure of the potential for the fully-correlated electron gas. Thus, from a quantum-mechanical viewpoint, the asymptotic structure of the image potential is due to Pauli-correlation effects. We also show^{27,38} that the potential W_x goes to a value of $-(2/3)$ (in units of $3k_F/2\pi$), the Kohn-Sham homogeneous electron gas result, in the interior of the metal.

The calculations in this chapter are performed employing accurate semi-analytical wavefunctions^{49,50} generated by a model effective potential. The accuracy of these wavefunctions is demonstrated by the

fact that they essentially reproduce³⁷ the results of fully self-consistent calculations^{51,52} performed within the local density approximation for the exchange-correlation energy. In the jellium model approximation of a metal surface, the positive ions are assumed to be smeared out to give a uniform positive charge background of density $\rho_+(x) = \bar{\rho} \theta(-x+a)$ beginning at the surface at $x = a$. Here $\bar{\rho} = k_F^3/3\pi^2$ is the bulk density, $k_F = 1/ar_s$, $a = (9\pi/4)^{1/3}$, is the Fermi momentum, and r_s is the Wigner-Seitz radius. Due to translational invariance in the plane parallel to the surface, the wavefunctions of an electron of momentum \mathbf{k} are of the form

$$\Psi_{\mathbf{k}}(\mathbf{r}) = -\sqrt{(2/V)} \phi_{\mathbf{k}}(x) e^{i\mathbf{k}_{\parallel} \cdot \mathbf{x}_{\parallel}} \quad , \quad (3.1)$$

where \mathbf{k}_{\parallel} and \mathbf{x}_{\parallel} are the momentum and position vectors in the plane parallel to the surface, k and x the corresponding quantities perpendicular to the surface, $\phi_{\mathbf{k}}(x)$ the component of the wavefunction in the direction of the inhomogeneity, and V the volume of the crystal. The component $\phi_{\mathbf{k}}(x)$ is generated by the local effective potential $V_{\text{eff}}(x)$ given by

$$V_{\text{eff}}(x) = Fx[\theta(x) - \theta(x-b)] + W \theta(x-b) \quad , \quad (3.2)$$

where F is the field strength and W the barrier height. These quantities can also be expressed in terms of the field strength and barrier height parameters x_F and b respectively as $F = (W/b) = (k_F^2/2)x_F$, where $(k_F^2/2)$ is the Fermi energy. This is the finite linear potential model⁴⁹. The linear potential model⁵⁰ for which $V_{\text{eff}}(x) = Fx \theta(x)$ is

a special case of this model potential. The solutions of the Schrodinger equation for the potential of Eq.(3.2) are

$$\varphi_k(x) = \begin{cases} \sin[kx + \delta(k)] & \text{for } x \leq 0 \\ B_k \text{ Ai}(\zeta) + C_k \text{ Bi}(\zeta) & \text{for } 0 \leq x \leq b \\ D_k \exp(-\kappa x) & \text{for } x \geq 0 \end{cases}, \quad (3.3)$$

where $k = \sqrt{2E}$, $\kappa = \sqrt{2(W-E)}$, $\zeta = (x - E/F)(2F)^{1/3}$, and E is the energy, and where $\text{Ai}(\zeta)$ and $\text{Bi}(\zeta)$ are the linearly independent solutions of the Airy differential equation.⁵³ The phase factor $\delta(k)$ and the coefficients B_k , C_k , and D_k are determined by the requirement of the continuity of the wavefunction and its logarithmic derivative at $x=0$ and $x=b$. The jellium edge position is determined either by charge neutrality or equivalently by the Sugiyama sum rule.^{54,55}

The wavefunctions described above are physically correct in that they are oscillatory in the bulk, give rise to appropriate Friedel oscillations of the density in the surface region, and are exponential in the classically forbidden region. For these wavefunctions, the spatial integrals for the majority of properties can be performed analytically.^{49,50} The expressions given in the following sections are in terms of the dimensionless variables $y = k_F x$, $y_{||} = k_F x_{||}$, $q = (k/k_F)$. The jellium edge, barrier height, and slope parameters are now $y_a = k_F a$, $y_F = k_F b$, and $y_b = k_F b$. With this change in variables, all the properties that are discussed below can be expressed in terms of universal functions of the slope and barrier height parameters. In terms of the new variables, a distance of $y=2\pi$ corresponds to a Fermi wavelength, which for Al is 3.59 Å and for Cs is 9.75 Å.

3.1 Structure of the Fermi Hole at Metallic Surfaces

In an attempt to obtain the structure of the image charge, Sahni and Bohnen³⁵ studied the behavior of the Fermi hole at metal surfaces. They discovered that as an electron is removed from the metal, its Fermi hole - unlike the image charge which is localized in the surface region - starts spreading into the interior of the crystal. The width of the hole depends upon the position of the electron and keeps increasing as the electron is pulled further and further out. Thus in the asymptotic limit, when the electron is very far from the surface, Sahni and Bohnen concluded that its Fermi hole would extend throughout the crystal. In arriving at their conclusions, Sahni and Bohnen studied only the behavior of the exchange charge density averaged over the planes parallel to the surface. Their analysis did not include details of the structure in these planes. Furthermore, their study extended upto electron positions of a maximum of approximately two Fermi wavelengths from the surface for typical density profiles. In this section we more emphatically demonstrate³⁴ the spreading of the Fermi hole through the volume of the crystal by considering electron positions upto approximately six Fermi wavelengths from the surface. In addition we study the structure of the Fermi hole in the plane perpendicular to the surface encompassing the axis of electron removal. We also make comparisons between the classical and quantum-mechanical charge distributions in the planes parallel to the surface. Finally by deriving an analytical expression for the exchange charge density deep in the bulk, we show that irrespective of the electron position the Fermi hole extends all the way to minus infinity.

With electronic wavefunctions of the form Eq. (3.1), the Fermi hole [Eq. (1.20)] at r' for an electron at r is given in terms of the dimensionless variables y , $y_{||}$, and q , with $R=|y_{||}|$, as (see Appendix B)

$$\frac{\rho_x(y, y', R)}{(\bar{\rho}/2)} = \frac{36}{\rho_n(y)} \left| \int_0^1 dq \phi_q^*(y) \phi_q(y') \frac{(1-q^2)^{1/2}}{R} \right. \\ \left. J_1\{(1-q^2)^{1/2}R\} \right|^2, \quad (3.4)$$

where $J_1(x)$ is the first-order Bessel function, and $\rho_n(y)$ is the density normalized with respect to the bulk value $\bar{\rho} = k_F^3/3\pi^2$;

$$\rho_n(y) = \frac{\rho(y)}{\bar{\rho}} = \int_0^1 dq (1-q^2) |\phi_q(y)|^2. \quad (3.5)$$

It is from Eq. (3.4) that we can study the charge distribution in planes parallel to the surface, spreading radially from the axis along which the electron is being removed. On substituting $y_{||} = 0$ in Eq. (3.4) we obtain the expression for the Fermi hole in the plane perpendicular to the surface and encompassing the axis of electron removal:

$$\frac{\rho_x(y, y', y_{||})}{\bar{\rho}/2} \Big|_{y_{||}=0} = \frac{9}{\rho_n(y)} \left| \int_0^1 dq (1-q^2) \phi_q(y) \phi_q(y') \right|^2. \quad (3.6)$$

In this section we perform our calculations using the wavefunctions generated by the linear potential model⁵⁰ of a surface. (For a similar study employing the step-potential model⁵⁶ wavefunctions, we refer the reader to our published work³⁴). For the linear potential model

$$\phi_k(x) = \sin[kx + \delta(k)]\theta(-x) + \sin\delta(k)\frac{\text{Ai}(-\zeta)}{\text{Ai}(-\zeta_0)}\theta(x) \quad , \quad (3.7)$$

with $\delta(k) = \cot^{-1}[\text{Ai}'(-\zeta_0)/(\zeta_0)^{1/2}\text{Ai}(-\zeta_0)]$, and where $\text{Ai}(\zeta)$ and $\text{Ai}'(\zeta)$ are the Airy functions and their derivatives, respectively; $\zeta = x(k_F^2/x_F)^{1/3} - \zeta_0$; $\zeta_0 = (k_F x_F)^{2/3} k^2/k_F^2$ and $F = (k_F^2/2)/x_F$. The density profile parameter is $y_F = k_F x_F$. For our calculations we choose $y_F = 3$, a typical⁵⁷ metallic density profile.

In Fig. 2 we plot the cross-section through the Fermi hole given by Eq. (3.6) for various positions of the electron outside the surface at $y=8, 20$ and 35 . It is clear from these graphs that as the electron moves further out from the surface, the Fermi hole begins to spread deeper into the crystal as the charge near the surface decreases. There is an order of magnitude decrease in the amplitude of the first peak as the electron is taken from $y=8$ to $y=35$. As a function of the distance into the bulk metal, although the amplitude of the succeeding peaks decreases, the oscillations continue for substantial distances into the metal. This structure of the Fermi hole is in sharp contrast with the classical image charge which has zero thickness and is localized at the jellium edge. The Fermi hole distribution is also significantly different from the classical distribution in the planes

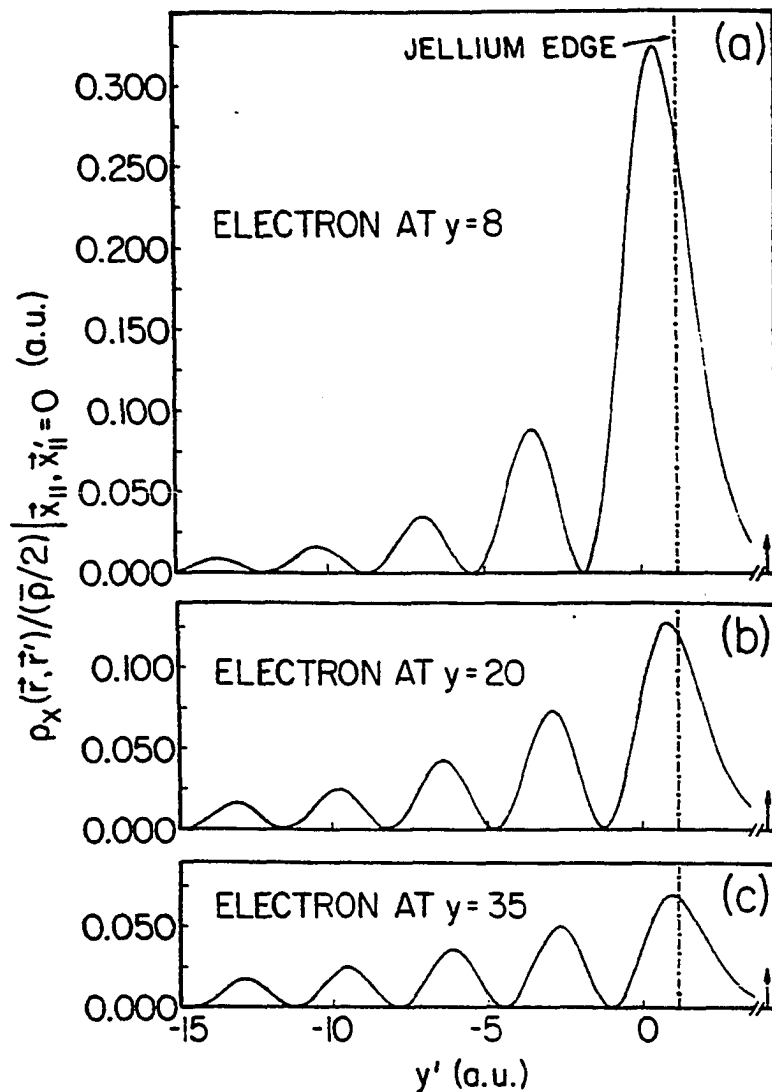


FIG. 2. Variation of the cross section of the Fermi hole $\rho_x(\mathbf{r}, \mathbf{r}')$ in the plane of electron removal perpendicular to the surface versus $y' = k_F x'$ for different positions y of the electron in the vacuum region. [See Eq. (3.6)].

parallel to the surface. This is shown in Fig. 3 where we plot the planar charge distribution of Eq. (3.4) in the planes at different y' for the same electron positions outside the metal as those in Fig. 2. Also shown with the dashed line is the distribution

$$\rho_x(y, y'; |y_{||}|) = \rho_x(y, y'; |y_{||}|=0) \frac{(y-y')^3}{[(y-y')^2 + |y_{||}|^2]^{3/2}}, \quad (3.8)$$

which is how the Fermi hole would look like if it had the same analytical form as the classical charge distribution. It is clear from the figure that the classical distribution bears little resemblance to the quantum-mechanical distribution. As a consequence of the differences between the shapes of the two charge distributions both in the direction perpendicular to the surface, as well as in the direction parallel to the surface, it is expected that the corresponding potentials would also be different. However, in the following sections we show that both the classical and the quantum-mechanical distributions, although fundamentally different, give rise to the same potential asymptotically far from the surface. Near the surface the classical approximation is not valid, and the classical potential is singular in contrast to the quantum-mechanical potential which goes to a finite value inside the metal.

In order to study how the exchange charge spreads asymptotically deep in the bulk, we derive in Appendix C the y' dependence of the planar averaged Fermi hole which is defined as

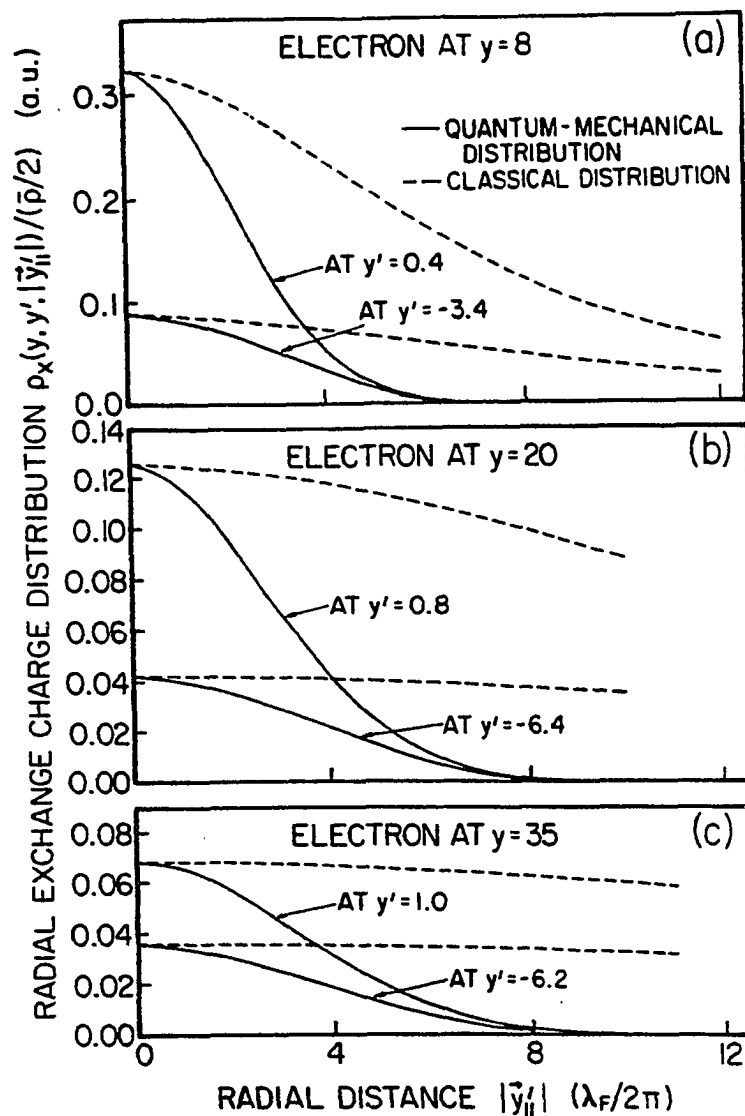


FIG. 3. Variation of the radial distribution of the Fermi hole charge density in planes at y' parallel to the surface versus the distance from the axis of electron removal [see Eq. (3.4)] for different positions y of the electron outside the surface. The solid lines correspond to the quantum-mechanical charge distribution and the dashed lines represent the classical distribution of charge. [See Eq. (3.8)].

$$\rho_x(y, y') = \frac{1}{A} \int dx_{||} \int dx'_{||} \rho_x(r, r') \quad , \quad (3.9)$$

where A is the surface area. In Appendix C we show that for arbitrary positions y of the electron, $\rho_x(y, y') \sim y'^{-2}$ for $y' \ll 0$. This derivation is independent of the model used to represent the effective potential at the surface. The implication here is that this will be the asymptotic dependence even in the case in which the surface potential is derived in a fully self-consistent manner.

That there is charge at $y' = -\infty$ can be seen by considering the center of mass of the Fermi hole. It is evident that the integral

$$\langle y' \rangle = \int_{-\infty}^{\infty} y' \rho_x(y, y') dy' \sim \ln|y'| \quad (3.10)$$

is weakly divergent in the limit $y' \rightarrow -\infty$. If there were no charge at minus infinity, or equivalently if the extent of the charge distribution were finite, the integral $\langle y' \rangle$ would converge. [We remind the reader here that the integral $\int_{-\infty}^{\infty} \rho_x(y, y') dy'$ does converge, and its value is unity. Also for the homogeneous electron gas, $\langle y' \rangle$ equals y]. Thus we see that there is a tail of the exchange charge density extending all the way upto minus infinity.

To see how much of the Fermi hole exists deep in the metal for asymptotic positions of the electron, we plot in Fig. 4 the amount of charge in the region $-y < y' < \infty$ versus the electron position y outside the crystal. Thus the charge in the region $-\infty < y' \leq -y$ is given by the difference between this curve and the horizontal line at unity which

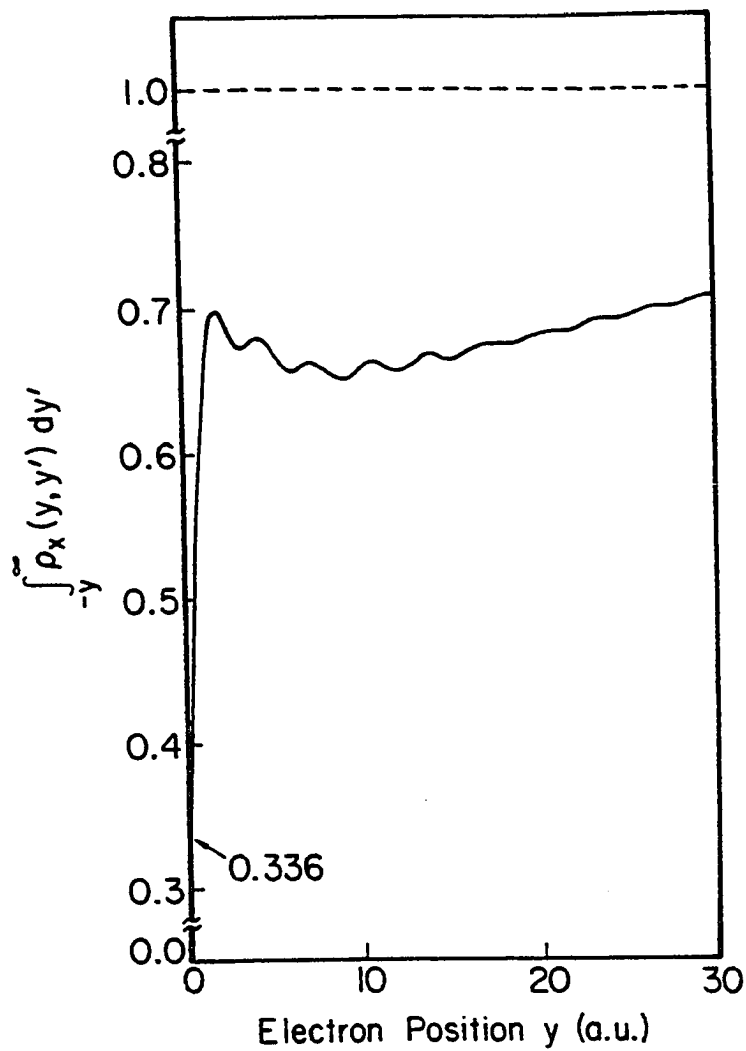


FIG. 4. Variation of the total exchange charge between $-y$ and ∞ as given by the integral $\int_{-y}^{\infty} \rho_x(y, y') dy'$ versus the electron position y .

represents the total exchange charge. It is evident from the graph that for an electron at $y=30$, which corresponds to a distance of approximately five Fermi wavelengths, there is about 30% of the total charge in the region $y' \leq -30$. Thus it is clear that the Fermi hole is not localized to the surface region and is spread throughout the crystal. Furthermore, the Fermi hole of an electron for this extended system is never stable and its structure changes with electron positions even for electrons asymptotically far from the surface.

3.2 Structure of the Slater Potential at Metallic Surfaces

In this section we determine the structure of the Slater²⁸ potential of Eq. (2.18) for the many-electron non-uniform system at jellium metal surfaces. The Slater potential would be the local effective potential seen by electrons if the Fermi hole were a static charge distribution. In terms of the dimensionless variables y , y' , and R , where $R = |y||y'|$, the Slater potential in units of its bulk value is given as³⁶

$$\frac{V_{\mathbf{x}}^{\text{Sl}}(y)}{(3k_{\text{F}}/2\pi)} = - \frac{8}{\rho_{\text{n}}(y)} \int_{-\infty}^{\infty} dy' \int_0^{\infty} dR \frac{R g(y, y', R)}{[R^2 + (y-y')^2]^{1/2}}, \quad (3.11)$$

where

$$g(y, y', R) = \left| \int_0^1 dq \phi_q^*(y) \phi_q(y') Q J_1(QR)/R \right|^2, \quad (3.12)$$

$Q = (1-q^2)^{1/2}$, $J_1(x)$ is the first-order Bessel function, and $\rho_n(y)$ is the electronic density normalized with respect to the bulk value $\bar{\rho} = k_F^3/3\pi^2$. The details of derivation are given in Appendix D.

An analytical expression for the Slater potential was originally derived by Juretschke⁵⁸ and more recently by others⁵⁹ for the analytical wavefunctions of the infinite barrier model.⁵ This model is a very poor representation⁵⁰ of the effective potential at a metal surface since it does not permit electrons to be removed beyond the barrier. Thus, the asymptotic structure of the Slater potential cannot be studied via the expression derived within the context of this model.

In Fig. 5 we plot $v_x^{S1}(y)/(3k_F/2\pi)$ as a function of the electron position y for a metal of bulk density $r_s=4$. The potential has been calculated using the wavefunctions of Eq. (3.3) generated by the finite linear potential model. The field strength and barrier height parameters for the wavefunctions are those determined by minimization of the surface energy within the local density approximation for exchange and correlation (see the Appendix of Ref. 37). The values of these parameters are $y_F=1.35$ and $y_b=2.58$, and the jellium edge is at $y_a=0.48$ for the bulk density of $r_s=4$. The range of the abscissa in the figure corresponds to a distance of about half a Fermi wavelength inside the metal to approximately two Fermi wavelengths outside. Inside, as expected, the potential exhibits a Friedel oscillation but tends to the incorrect value of -1 in the bulk. In the region outside the metal we also plot for purposes of comparison the image potential,

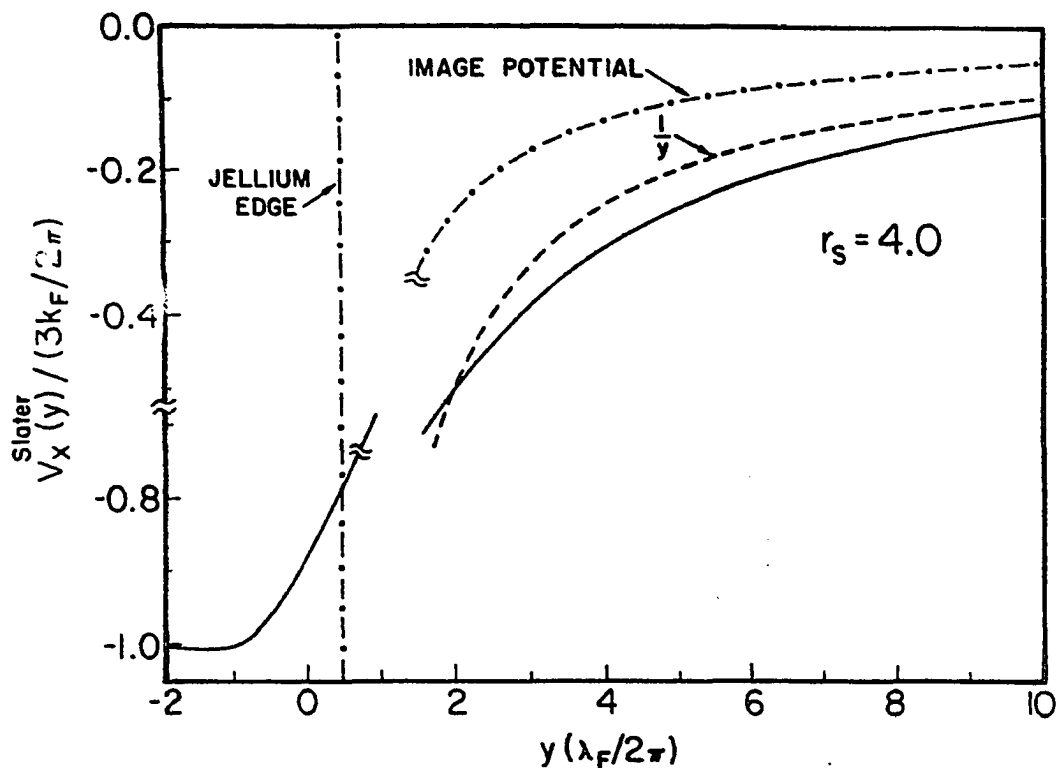


FIG. 5. Variation of the universal function $V_x^{Sl}(y)/(3k_F/2\pi)$, where $V_x^{Sl}(y)$ is the Slater potential [see Eq. (3.11)], versus the electron position y . The function $1/y$ and the image potential $(\pi/6)/y$ are also plotted.

which in terms of the variables used here is $(\pi/6)/y$, as well as the function $1/y$. It is clear from the figure that the Slater potential is distinctly different from the image potential. However, it appears to be approaching $1/y$, which in terms of the electron distance x translates to $(3/2\pi)/x = 0.48/x \approx 1/2x$. To study the asymptotic structure of the Slater potential, we plot in Fig. 6 the potential on a logarithmic scale upto about eight Fermi wavelengths from the surface. It is evident from this figure that asymptotically the Slater potential does closely approximate the function $1/y$, and is not the image potential. Thus asymptotically, the Slater potential is image-like but with a coefficient that is twice as large as the image potential coefficient.

We conclude this section by reiterating that the Slater potential is determined by ignoring the fact that the Fermi hole changes its structure as a function of the electron position. Further, we note that if the electrostatic potential were calculated from the classical image charge by ignoring the change in its distribution as a function of the position of the test charge, the resulting potential would also be image-potential-like but with a coefficient twice as large. However, if the electric field due to the classical charge is first determined and then integrated to calculate the work done in moving the charge in this field, the dynamic nature of the image charge is properly accounted for and the resulting potential is indeed the image potential. Our physical interpretation of the Kohn-Sham effective potential is based precisely on the manner described above to take into account the change in the structure of the Fermi-Coulomb hole

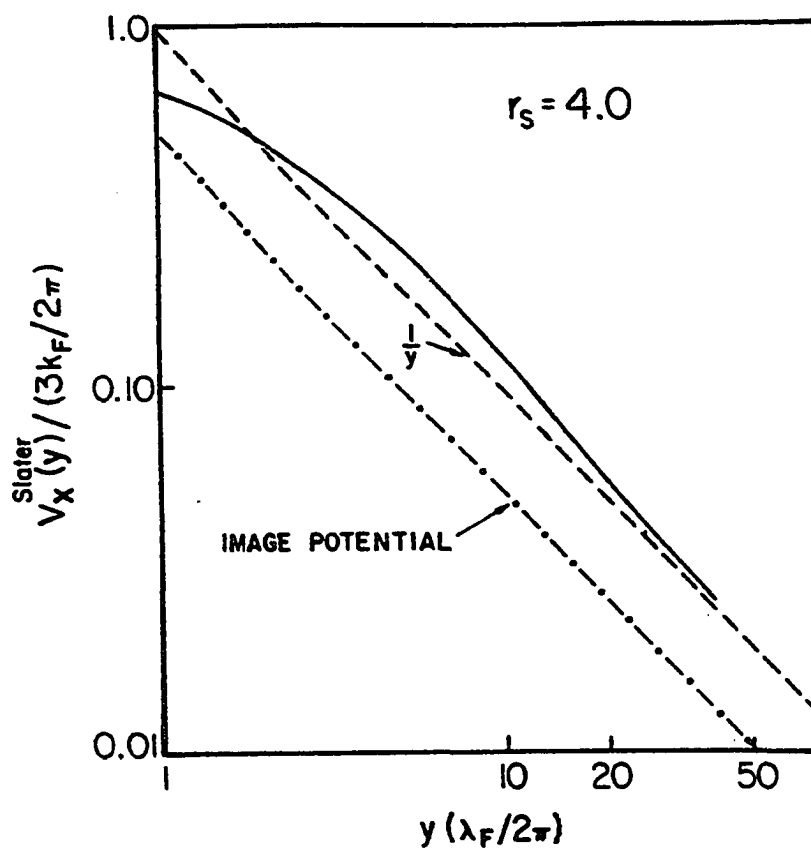


FIG. 6. Variation of the universal function $V_x^{Slater}(y)/(3k_F/2\pi)$, where $V_x^{Slater}(y)$ is the Slater potential [see Eq. (3.11)], for asymptotic positions y of the electron outside the surface. The function $1/y$ and the image potential $(\pi/6)/y$ are also plotted.

charge distribution as a function of the electron position. We show in the next section how through this interpretation the effective potential at a metal surface is asymptotically the image potential, and that it also approaches the correct Kohn-Sham homogeneous electron gas value in the bulk.

3.3 Structure of the Potential W_x at Metallic Surfaces

As discussed in Chapter two (sect. 2.1), a consequence of our interpretation²⁷ of the Kohn-Sham exchange-correlation potential is that the quantum-mechanical origin of the asymptotic structure of the effective potential of any interacting electron gas system is the same and due entirely to Pauli correlation effects. In this section we show³⁸ that the effective exchange potential W_x at metallic surfaces as determined from the delocalized Fermi hole (sect. 3.1) goes as the image potential $-(1/4x)$ asymptotically far from the surface. Further, we show that for electrons in the bulk, the exchange potential W_x goes to a value of $-(2/3)$ (in units of $3k_F/2\pi$) as it must according to the Kohn-Sham theory.

As in the case of the Slater potential, we perform our calculations in the jellium model approximation using the wavefunctions [Eq. (3.3)] generated by the finite linear potential model.⁴⁹ We consider high bulk density systems corresponding to a Wigner-Seitz radius of $r_s=1.0$ and $r_s=2.0$. For high density systems, the model potential wavefunctions most closely approximate³⁷ those of fully-self-consistent calculations as performed within the local density approximation for exchange and correlation. In particular the

amplitude of the Friedel oscillations of both the electronic density as well as the effective potential for the high density systems is very small and therefore represented well by the model effective potential wavefunctions. The field strength and barrier height parameters, taken from the Appendix of Ref. 37, are $y_F=5.88$ and 3.38 , and $y_b=6.02$ and 4.25 for $r_s=1.0$ and 2.0 respectively. The jellium edge positions are at $y_a=2.37$ and 1.33 .

We first study the electric field due to the Fermi hole as a function of the electron position. For an electron at y , the electric field is given by (see Appendix E)

$$\frac{\epsilon_x(y)}{(3k_F^2/2\pi)} = - \frac{8}{\rho_n(y)} \int_{-\infty}^{\infty} dy' \int_0^{\infty} dR \frac{R g(y, y', R)}{[R^2 + (y-y')^2]^{3/2}} (y-y'), \quad (3.13)$$

and is in the direction perpendicular to the surface. The quantities $\rho_n(y)$ and $g(y, y', R)$, and the variables y , y' and R are the same as defined in the previous sections. In Fig. 7 we plot the electric field in units of $(3k_F^2/2\pi)$ for $r_s=2.0$ as a function of the electron position. The electric field is maximum near the surface region and it vanishes for electron positions inside the metal exhibiting Friedel oscillations. Outside the surface the electric field also decays. Its asymptotic form is shown in Fig. 8 for a distance upto approximately eight Fermi wavelenghts outside the surface. In this figure we also plot the function $1/2y^2$ which translates in terms of the original variables to $(3/4\pi)/x^2 = 0.24/x^2 \approx 1/4x^2$, the image electric field. It is clear from the figure that from about $y=35$ onwards, the electric

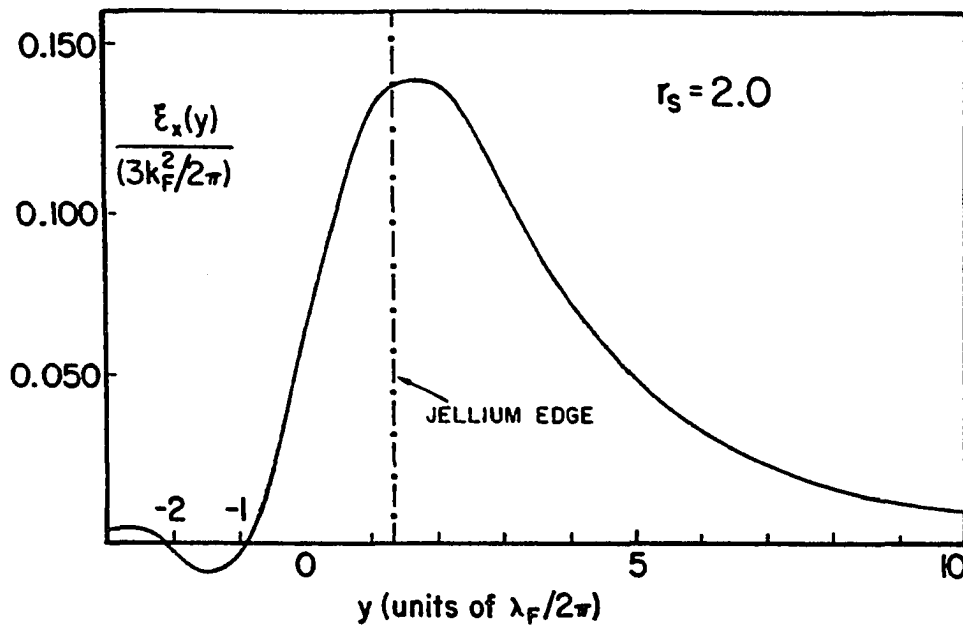


FIG. 7. Variation of the universal function $\epsilon_x(y)/(3k_F^2/2\pi)$, where $\epsilon_x(y)$ is the electric field due to the Fermi hole [see Eq. (3.13)], versus the electron position y .

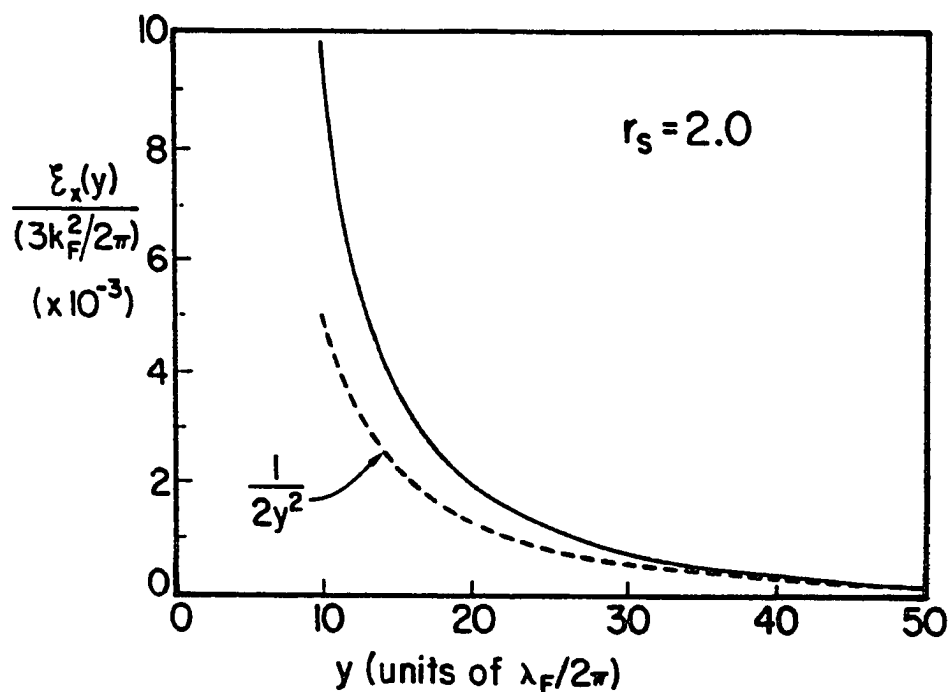


FIG. 8. Variation of the universal function $\epsilon_x(y)/(3k_F^2/2\pi)$, where $\epsilon_x(y)$ is the electric field due to the Fermi hole [see Eq. (3.13)], for asymptotic positions y of the electron outside the surface. The function $1/y^2$ is also plotted.

field is essentially the same as the image field. Thus the line integral of the electric field which is W_x is then $-(1/4x)$, the image potential. To demonstrate this explicitly, we plot in Fig. 9 the universal function $W_x/(3k_F/2\pi)$ which is (see Appendix E)

$$\frac{W_x(y)}{(3k_F/2\pi)} = 8 \int_{-\infty}^y \frac{dy'}{\rho_n(y')} \int_{-\infty}^{\infty} dy'' \int_0^{\infty} dR \frac{R g(y', y'', R)}{[R^2 + (y' - y'')^2]^{3/2}} (y' - y'') \quad (3.14)$$

for the same electron positions as in Fig. 8 along with the function $-(1/2y) = -(0.24/x) \approx -(1/4x)$. It is evident that the two curves merge, thereby clearly demonstrating that for asymptotic positions of the electrons the potential W_x is the image potential. Thus, when looked at quantum-mechanically, the image potential, which is the effective potential for electrons asymptotically far from the surface, is due to the Fermi hole which in turn is a consequence of the Pauli exclusion principle.

Thus we see that the quantum-mechanical interpretation of the asymptotic structure of the image potential as due to Pauli correlation effects is consistent with the classical picture of the image potential being a consequence of the Coulomb interaction between a test charge and its image charge. Classically, the image potential is due to the induced image charge which is the response of the metal surface to the external test charge. For positions asymptotically far from the surface an electron may be considered as a distinguishable classical particle and the charge induced by it on the surface determined. Thus, treating the electron as an external point charge, Lang

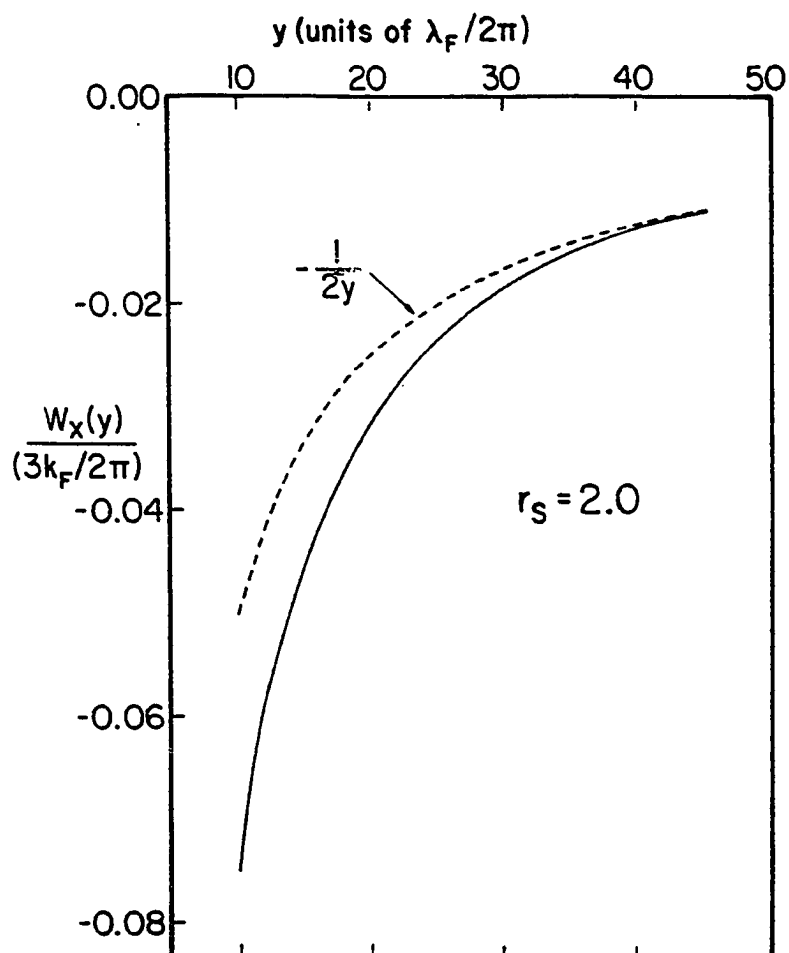


FIG. 9. Variation of the universal function $W_x(y)/(3k_F/2\pi)$, where $W_x(y)$ is the work done against the electric field $\epsilon_x(y')$ due to the Fermi hole [see Eq. (3.14)], versus the electron position y . The function $-1/2y$ is also plotted.

and Kohn^{51,52,60} have calculated the induced charge distribution within linear response theory and shown the energy of interaction to be $-[1/4(x-x_0)]$, where x_0 is the center of mass of the induced charge. The induced charge has also been shown^{33,60} to have the same structure as the classical image charge in the planes parallel to the surface. The image potential at metallic surfaces has also been derived^{46,47,61,62} by consideration of the asymptotic structure of the Kohn-Sham exchange-correlation potential $\mu_{xc}(\mathbf{r})$. In these derivations the distant electron in the vacuum is also treated as a point charge distinct from the electronic gas of the metal and independent of the inhomogeneity at the surface. On the other hand, from a quantum-mechanical viewpoint this electron is part of the interacting N -electron system, and treated as such in the present formalism. The electron is not treated as an external charge and there is, therefore, no induced charge. The Fermi-Coulomb hole of an electron is not an induced charge distribution but rather an intrinsic property of the system itself which contributes to the effective potential. We have determined the effective potential from the wavefunctions themselves, and shown that quantum-mechanically too its asymptotic structure is the image potential. The fact that both classical and quantum theories lead to the same asymptotic structure implies that the interpretations of each formalism are equally valid.

In the discussion above we studied the structure of the potential W_x for electrons asymptotically far from the surface. We next wish to obtain the value this potential approaches in the metal bulk relative to the vacuum level which is assumed to be at zero potential. For

this we calculate the work done as an electron is removed from inside the metal to distances infinitely far from the surface. In Table I we show for a metal of bulk density $r_s=1.0$, the incremental work ΔW_x done on an electron as it is pulled out of the metal from $y=-5$ to $y=30$ in various increments of distances. We notice that the work done is maximum when the electron is taken from $y=1.0$ to $y=5.0$. This is expected as the electric field due to the Fermi hole is maximum in this region. (Note that the metal surface is at $y_a=2.37$). We further note that as the electron distance from the surface increases, $\Delta W_x = W_x(y_{\text{final}}) - W_x(y_{\text{initial}})$ rapidly approaches $[(1/2y_{\text{initial}}) - (1/2y_{\text{final}})]$. This shows that asymptotically the potential is converging to $-(1/2y)$ [$\equiv -(1/4x)$], the image potential. The total work in removing the electron to infinity is obtained by adding $1/60$ to $W_x(30) - W_x(-5)$, as by $y=30$ the potential W_x is essentially the same as the image potential. Thus we obtain $W_x(\infty) - W_x(-5) = 0.669 \approx 2/3$ which, as discussed above, is the Kohn-Sham homogeneous electron gas value. Thus the potential W_x not only gives the correct asymptotic structure of the potential outside the metal but also leads to the correct quantum-mechanical value inside. We reiterate that the asymptotic structure of the Slater potential is $-(1/y)$, which is image-potential-like but with a coefficient twice as large as that of the image potential, and the value it approaches inside the metal is 1.0 which is one and a half times larger than the quantum-mechanical result. On the other hand, the exchange potential as determined⁵¹ within the local density approximation decays exponentially as a function of the electron distance outside the surface. However, the difference between the vacuum and metal interior values is given

TABLE I

Work W_x (in units of $3k_F/2\pi$) done against the electric field of the Fermi hole of an electron as it is removed from inside the metal to asymptotic distances outside the surface. The numbers shown here correspond to a metal with bulk electronic density of $r_s = 1.0$.

y_{initial}	y_{final}	ΔW_x	$W_x = \Sigma \Delta W_x$
-5.0	0.0	0.01196	0.01196
0.0	1.0	0.04379	0.05575
1.0	5.0	0.32752	0.38327
5.0	10.0	0.19636	0.57963
10.0	15.0	0.04570	0.62533
15.0	20.0	0.01641	0.64174
20.0	25.0	0.00742	0.64916
25.0	30.0	0.00358	0.65274

$$\Delta W_x(-5.0 \rightarrow \infty) = 0.65274 + (1/60) = 0.66941$$

correctly by this approximation because it is exact for the homogeneous electron gas in the metal bulk. Thus we see that the potential W_x not only has an asymptotic structure outside the metal which is in agreement with classical physics, but that as it approaches the metal bulk, it is lowered by the correct amount due to the exchange effects.

The wavefunctions of the finite linear potential model of a surface are very accurate for high bulk density systems and become more accurate as the density increases. For lower density metals, the model potential does not possess the requisite large Friedel oscillations which exist near the surface, and consequently the corresponding wavefunctions are not as accurate as those that might be obtained self-consistently. As such the results for the difference $W_x(\infty) - W_x(-\infty)$ for low density metals approximate less well the correct $2/3$ value. For example for $r_s=4.0$, this difference is 0.783 whereas for $r_s=2.0$ it is 0.719. As shown above, the result for $r_s=1.0$ is 0.669. For fully-self-consistent calculations of the W_x potential at surfaces, this difference will be exactly $2/3$ irrespective of the density of the metal. However, such a self-consistent calculation for the many-electron problem at surfaces would be a numerical tour de force since the Fermi hole charge is not localized to the surface but is spread throughout the crystal. In particular for asymptotic positions of the electron, a significant fraction of the Fermi hole lies, as discussed in sect. 3.1, many tens of Fermi wavelengths deep in the bulk. This charge must be accounted for precisely if accurate results are to be obtained. On the other hand, such a calculation can be performed easily for atomic systems because the Fermi hole is

localized within the atom, and therefore the potential W_x can be determined self-consistently for all electron positions without any numerical difficulty. The results of fully-self-consistent calculations for the ground-state energy and highest occupied eigenvalues of atoms with closed subshells are presented in the following chapter.

Chapter IV

**GROUND-STATE ENERGIES AND HIGHEST OCCUPIED EIGENVALUES OF ATOMS
IN EXCHANGE-ONLY APPROXIMATION (SELF-CONSISTENT APPLICATION)**

To demonstrate the applicability of the interpretation for the local exchange potential, we present in this chapter the results of fully self-consistent calculations³⁹ for the ground-state energies and the highest occupied eigenvalues of closed subshell atoms in the exchange-only approximation. Since the wavefunctions in this formalism are obtained from a local potential, the total energies must be an upper bound to the Hartree-Fock energies. On the other hand, with this interpretation, we know that the asymptotic structure of the exchange-correlation potential for the fully-correlated system is given²⁷ exactly by the exchange potential alone. Thus the highest occupied eigenenergies, which depend principally on the structure of the potential in the regions beyond the inner shells, should approximate well the non-relativistic ionization potential. We point out here that the same arguments for the highest occupied orbital energies cannot be applied to other exchange-only calculational schemes, such as Hartree-Fock² theory or the Optimized Potential Method,^{30,31} which are based on the variational principle for the energy. In these schemes, with a Slater-determinant-type wavefunction, either the orbitals or the potentials are optimized to minimize the energy. There is, therefore, no direct link between the exchange potential thus obtained and the exchange-correlation potential of fully-correlated systems. Thus, although for finite systems, the energies obtained in these exchange-only schemes too give an upper

bound to the true total ground-state energy, the corresponding highest occupied orbital energies are not directly related to the ionization potential as is the case for the present formalism. As such we compare the ground-state energies of the present work³⁹ to those of Hartree-Fock theory,² and the highest occupied eigenenergies to experimental⁴⁰ ionization potentials.

4.1 Ground-State Energies

In Table II we present results for the ground-state energies of the first ten atoms of the periodic table that have closed subshells, together with the Hartree-Fock values.² The reason for comparing the total energies with the corresponding Hartree-Fock values is that the latter is the lowest possible energy a system can have in the exchange-only approximation in which only Pauli-correlations between the electrons are incorporated in the wavefunction. The results presented here are obtained³⁹ by solving Eq. (2.4b) self-consistently with $W_c = 0$. The expression for the potential W_x for the Ar atom in terms of the orbitals is given in Appendix A, and can easily be generalized for the other atoms discussed here. With the exception of the Be atom, for which the W_x -formalism value differs by 0.014%, the results for the remaining atoms lie within 50ppm of those of Hartree-Fock theory. For Kr and the heavier atoms, these differences are less than 10ppm. Further, as discussed earlier, the energies consistently lie above those of Hartree-Fock as they must. The self-consistency procedure for the determination of the local potential W_x is also numerically easier than that for the orbital-dependent potentials of Hartree-Fock theory.

TABLE II

Ground State atomic energies in the Pauli-correlated approximation. The negative values of the energies in atomic units are quoted.

ATOM	HARTREE-FOCK ^a	OPM ^b	PRESENT WORK ^c
Be	14.573	14.572	14.571
Ne	128.547	128.545	128.542
Mg	199.615	199.612	199.606
Ar	526.818	526.812	526.804
Ca	676.758	676.752	676.743
Zn	1777.848	1777.833	1777.820
Kr	2752.055	2752.042	2752.030
Sr	3131.546	3131.532	3131.519
Cd	5465.133	5465.112	5465.093
Xe	7232.138	7232.119	7232.101

a. See Ref. 2

b. See Ref. 31

c. See Ref. 39

4.2 Highest Occupied Eigenenergies

In Table III the results for the highest occupied orbital eigenenergies together with those of Hartree-Fock theory² as well as the experimental⁴⁰ ionization potentials are presented. We group those atoms whose last occupied subshell is an s subshell separately from the noble gas atoms. The reason for the separation is that the experimental ionization potentials for the former group lie below those of Hartree-Fock theory whereas for the latter they lie above. The W_x -formalism eigenvalues, with the exception of Ne, also lie above those of Hartree-Fock for the noble gas atoms, and below Hartree-Fock for the others. Thus, as predicted, the eigenenergies obtained in the present work do more closely approximate the experimental ionization potentials. Further, since the eigenenergies are a fair approximation to experiment, it can be inferred that the local potential W_x , which is the true (fully-correlated) effective potential asymptotically, is also accurate in the regions much closer to the atom. Of course, the experimental values include relativistic contributions. Also, the highest occupied eigenenergies of Hartree-Fock theory cannot be compared with the experimental removal energies since Koopmans's theorem⁶³ is valid⁶⁴ only for unrelaxed orbitals. However, the comparison with experiment does demonstrate how principal the contributions of Pauli-correlations are.

4.3 Comparison with the Optimized Potential Method Results

Finally, in this section we compare our results with those of the Optimized Potential Method^{29,30} (OPM) as obtained by Talman et al.^{30,31} The Talman et al ground-state energies are superior to those

TABLE III

Highest occupied eigenvalues of atoms in the Pauli-correlated approximation and experimental ionization potentials. The negative values of the energies in Rydbergs are quoted.

ATOM	HARTREE-FOCK ^a	OPM ^b	PRESENT WORK ^c	EXPERIMENT ^d
Be	0.619	0.617	0.626	0.685
Mg	0.506	0.504	0.521	0.562
Ca	0.391	0.389	0.402	0.449
Zn	0.585	0.577	0.646	0.690
Sr	0.357	0.355	0.369	0.419
Cd	0.530	0.533	0.583	0.661

Ne	1.701	1.691	1.713	1.585
Ar	1.182	1.171	1.178	1.158
Kr	1.048	1.003	1.035	1.029
Xe	0.915	1.033	0.899	0.892

a. See Ref. 2

b. See Ref. 31

c. See Ref. 39

d. See Ref. 40

of the present work; they also lie above Hartree-Fock, but differ from it by approximately half the difference between the present and the Hartree-Fock values. (See Table II). Since the OPM is a scheme to minimize the Hartree-Fock energy, the Talman orbitals are very close to those of Hartree-Fock theory. As a consequence, the Talman highest occupied eigenvalues also generally approximate well the Hartree-Fock results, and therefore are not as close to the experimental values as those of the present work. (See Table III). To compare the potentials, we plot in Figs. 10 and 11 the optimized exchange potential along with the self-consistently determined W_x potential for the Xe atom. As in the case of the potential W_x (Fig. 1) determined by employing non self-consistent wavefunctions, discussed in section 2.3, here too the two potentials are essentially equivalent in the shell regions of the atom and differ only in the intershell regions where the optimized potential possesses bumps. These bumps are yet to be interpreted physically but arise because the energy is being forced to be minimized. The fact that these bumps in the optimized potential lead to an energy lower than that of the present work may be explained on the basis of the virial theorem. Because of the bumps, the OPM potential is more confining for the electrons than the W_x potential. Thus, by the uncertainty principle, the OPM potential leads to a higher kinetic energy for the electrons. Now according to the virial theorem, the total energy is equal to the negative of the kinetic energy, and therefore the total energy in the OPM potential must be lower than that in the W_x -formalism. (Although the Slater potential is more confining (see Fig. 1), these arguments are inapplicable to this potential since it does not satisfy the virial theorem). The OPM

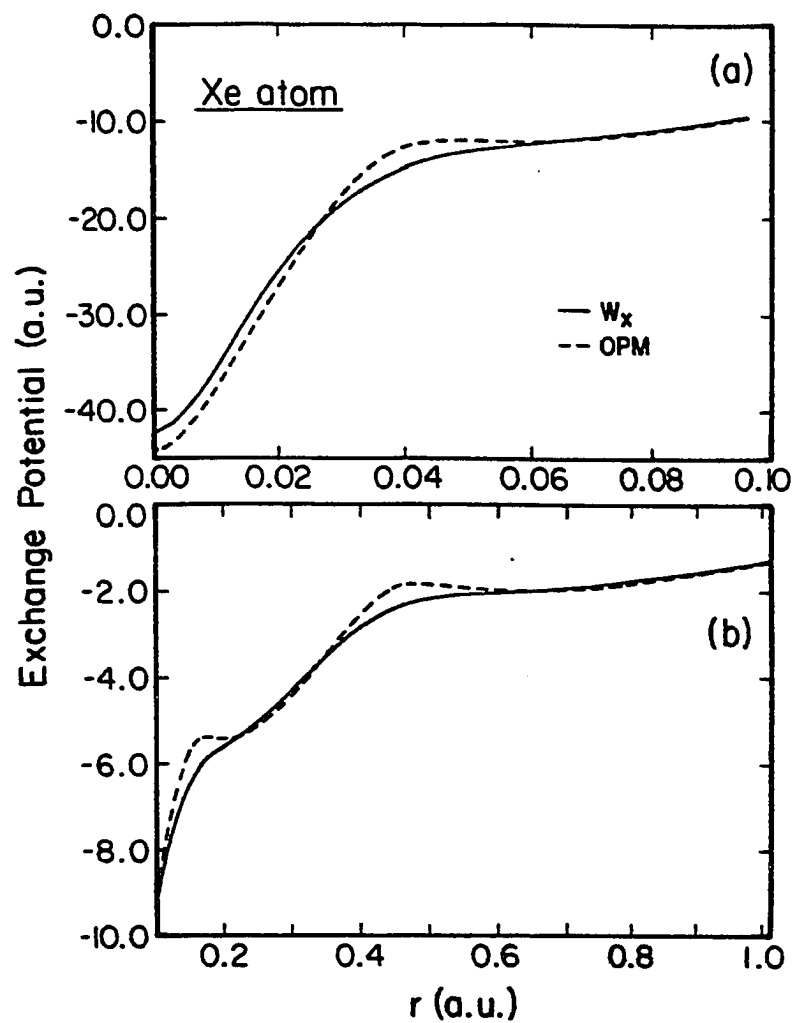


FIG. 10. The self-consistently determined W_x and the Optimized Potential Method (OPM) potentials for the Xenon atom in the interior of the atom.

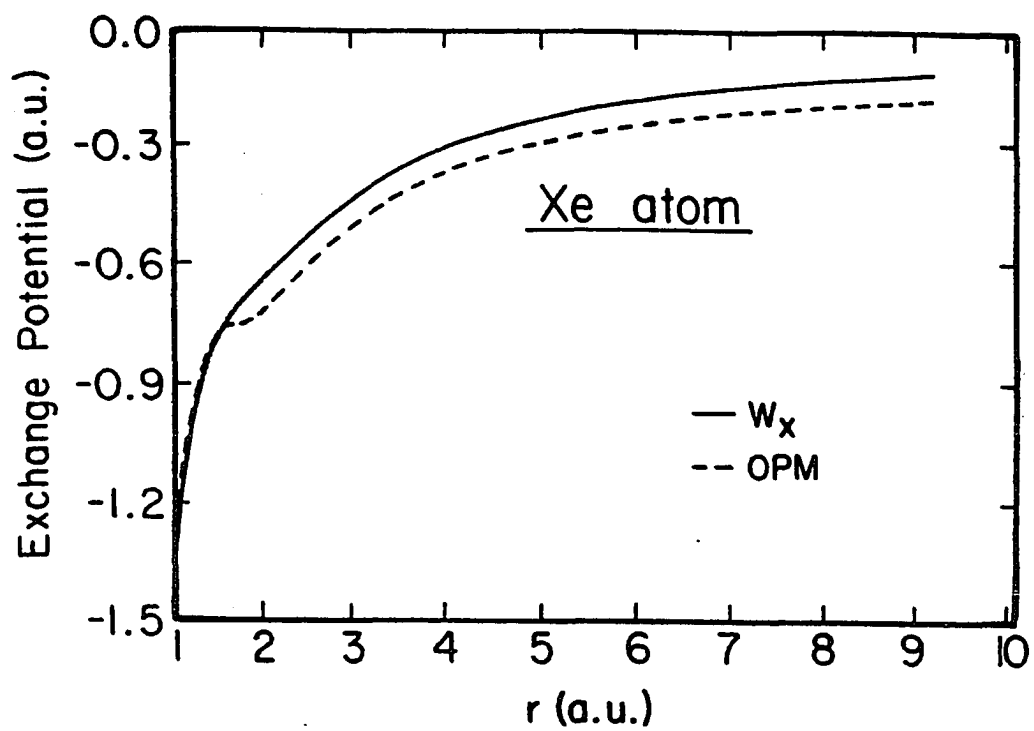


FIG. 11. The self-consistently determined W_x and the Optimized Potential Method (OPM) potentials for the Xenon atom in the region exterior to the shells.

ground-state energies are lower than those of the present work by 25ppm. On the other hand, because of these bumps, the OPM highest occupied eigenenergies are not as close to the experiment as those obtained in the present work. For electrons asymptotically far from the nucleus, Talman and Shadwick³⁰ have proved analytically that the OPM potential should go as $-(1/r)$. However, the potential calculated numerically for the Xe atom (see Fig. 11) by Talman et al,³² is not $-(1/r)$ even for distances as far out as nine atomic units from the nucleus. The same trend is observed for other atoms also. Sometimes the OPM potential lies above and sometimes below $-(1/r)$. This is a manifestation of the complexity involved in solving the OPM equations numerically. This complexity is further demonstrated by the fact that the OPM potentials as obtained by Talman et al generally do not satisfy²⁷ the virial theorem based sum rule of Eq. (1.32), which in principle²¹ they must. For example, as pointed out in section 2.3, when we substitute the Talman orbitals for the Ar atom in Eq. (1.32), the left and right hand sides of the sum rule differ and are -60.32 Ry. and -59.94 Ry. respectively. On the other hand, the potential W_x for Xe (Fig. 11) does go as $-(1/r)$ from about four atomic units onwards. Furthermore, in addition to satisfying the sum rule of Eq. (1.32) analytically, it also satisfies³⁹ the sum rule numerically, thus demonstrating the numerical ease of these calculations. In Table IV we compare the exchange energies $E_x[\Psi_i]$ as determined from the orbitals with those obtained from the potential W_x employing the expression from the right hand side of the virial theorem sum rule. The sum rule is satisfied consistently to 6-8 significant figures. However, since the OPM leads to energies lower than those obtained in

TABLE IV

Comparison of the exchange energies $E_x[\Psi_i]$ in atomic units as determined from the orbitals Ψ_i with those obtained from the potential W_x as given by the expression on the right hand side of the virial theorem sum rule [Eq. (1.32)].

ATOM	$-E_x[\Psi_i]$	$\int \rho(\mathbf{r}) \mathbf{r} \cdot \nabla W_x(\mathbf{r}) d\mathbf{r}$
Be	2.6664683	2.6664679
Ne	12.1218322	12.1218313
Mg	16.0034424	16.0034413
Ar	30.1887921	30.1887905
Ca	35.2140002	35.2139984
Zn	69.6218314	69.6218286
Kr	93.8634786	93.8634751
Sr	101.9611276	101.9611240
Cd	148.8799536	148.8799497
Xe	179.0920564	179.0920524

the W_x -formalism, it implies that according to the current definition^{10,14} of exchange-only density-functional theory, the potential W_x is not the Kohn-Sham exchange potential μ_x . Nevertheless, the results for the total energies and highest occupied eigenvalues clearly demonstrate the high accuracy of this potential.

We conclude this chapter by noting that both the Hartree-Fock and the OPM theories are founded in the variational principle for the energy. The present formalism on the other hand is formulated entirely on the basis of physical considerations. The accuracy of the results presented here and those for metallic surfaces discussed in Chapter III, together with the fact that the potential W_x satisfies the virial theorem sum rule as well as the scaling laws, is all the more remarkable in light of these differences.

Chapter V

CONCLUSION

The time-independent Schrodinger equation provides the basis for calculating all the stationary-state properties of a many-electron system. However, the Schrodinger equation for a many-electron system can be solved only in an approximate manner. Further, it falls short of providing any intuitive picture of how the electronic motions are correlated. Slater²⁸ was the first to provide such an insight by suggesting that in Hartree-Fock theory each electron could be thought of as moving in the Hartree potential as well as the electrostatic potential produced by its orbital-dependent Fermi hole charge distribution. Slater simplified²⁸ the picture by taking an average of the orbital-dependent Fermi holes, and then calculated a potential from this averaged Fermi hole. Thus, the ad hoc potential proposed by Slater was a local effective potential. The work of Slater, in addition to providing a physical interpretation, thus reduced the complexity of solving the Hartree-Fock equations to that of the Hartree equations.

Following the work of Slater, Hohenberg, Kohn and Sham^{7,9} were able to prove rigorously that all the properties of an interacting many-electron system could in fact be obtained by an equivalent system of non-interacting electrons in a local effective potential. The many-body component of this potential is derived by application of the variational principle for the energy to be the functional derivative of an unknown exchange-correlation energy functional of the density.

Thus, over the past two and half decades, the principal thrust of density-functional theory research has been towards the accurate approximation of this unknown energy functional, from which the local exchange-correlation potential is then obtained. It is only for the homogeneous electron gas that the exchange energy functional can be written explicitly in terms of the density, and the value of the exchange potential that is obtained⁹ from density-functional theory is two-thirds that of the Slater potential. Thus although the Hohenberg-Kohn-Sham theory makes the rather profound leap of reducing an intrinsically non-local problem to one that is local, it provides no physical insight into the structure of this local potential for an inhomogeneous system. On the other hand, the unknown exchange-correlation energy functional can be interpreted¹¹⁻¹³ as the energy of interaction between an electron and its Fermi-Coulomb hole. Furthermore, the highest occupied orbital eigenenergy^{16,17} of Kohn-Sham theory is minus the ionization energy. However, without an accurate knowledge of the local many-body potential, neither the ground-state energy nor the ionization potential can be obtained accurately.

In this thesis we have provided a physical interpretation for the local exchange-correlation potential in which the electrons move. We interpret it as the work required to move an electron against the electric field of its Fermi-Coulomb hole charge distribution. The Fermi-Coulomb hole is a fundamental property of an interacting electronic system, and from it both the exchange-correlation energy as well as the corresponding local potential can now be obtained

directly. Thus, with this interpretation, the requirement of Kohn-Sham theory of having to determine functional derivatives is obviated. The interpretation also explains on the basis of physical considerations why the Slater potential is incorrect. We have demonstrated the correctness of the physics underlying the interpretation, its universality, and the accuracy of the potentials obtained from it by applying the formalism to both few-electron atomic as well as many-electron metal surface non-uniform systems.

For closed subshell atoms in the exchange-only approximation^{10,14} the total ground-state energies lie, except for Be, within 50 ppm of those of Hartree-Fock theory. (For Be the difference is 0.014%). Since the asymptotic structure of the exchange-correlation potential within our formalism is that of the exchange-only case, the corresponding highest occupied orbital eigenenergies of these atoms closely approximate the experimental ionization potentials. For the same reason the asymptotic structure of the potential in atoms goes as $-(1/r)$ whereas that for metallic surfaces it is the image potential $-(1/4x)$. This also demonstrates the intrinsic consistency of the formalism in that the asymptotic structure of the exchange-correlation potential for any inhomogeneous electronic system is due to the same (Pauli exclusion principle) effect. Furthermore, the exchange potential at metal surfaces goes to the correct Kohn-Sham value in the metal bulk.

From a purely theoretical viewpoint, our interpretation of the local exchange-correlation potential has also been shown to lie within

the rubric of Kohn-Sham density-functional theory. For example, in the exchange-only approximation,^{10,14} the potential W_x satisfies all scaling properties²¹ that the exact exchange potential must satisfy. It is also the only physically derived local potential known that satisfies analytically (and numerically as shown for the case of atoms) the virial theorem sum rule²¹ in orbital form. Other potentials that satisfy this sum rule do so in an approximate manner in that it is the approximate energy functionals and their derivatives that are employed in the expression. The Slater potential scales properly but does not satisfy the virial theorem sum rule.

Although in the formalism proposed by us the exchange-correlation potential seen by electrons is local, it differs in many significant ways from Kohn-Sham theory. For one, our theory is not founded in the variational principle for the energy, but rather on physical arguments that account for the fact that the motion of electrons is correlated due to the Pauli exclusion principle and Coulomb repulsion. Thus, for example, the thrust of exchange-only^{10,14} Kohn-Sham theory is a search for that local potential whose orbitals minimize the Hartree-Fock energy. On the other hand, the orbitals in our formalism are derived from a potential that arises naturally as a consequence of the Pauli exclusion principle which keeps electrons of parallel spins apart. Thus, in our formalism, the exchange-only approximation means that we approximate the full exchange-correlation potential by its exchange component. Therefore, the potential thus obtained is not the exact (optimum) exchange potential of exchange-only^{10,14} Kohn-Sham theory. The fact that the ground-state energies for atoms in our formalism

differ from those of the Optimized Potential Method by only 25 ppm speaks to the correctness of the physics invoked. That the exchange potential in our formalism is a part of the full exchange-correlation potential, and is indeed the exact effective potential for asymptotic positions of the electron, is further demonstrated by the fact that the highest occupied orbital eigenenergies of atoms as obtained in our work closely approximate the experimental ionization potentials. On the other hand, the highest occupied eigenvalues of exchange-only Kohn-Sham theory have no physical significance and cannot be interpreted as removal energies. They tend to approximate well the eigenvalues obtained in Hartree-Fock theory. This is yet another significant way in which our theory differs from exchange-only Kohn-Sham theory. As opposed to both Hartree-Fock and exchange-only density-functional theories, our theory in the Pauli-correlated approximation is not distinct from but intrinsically a part of the fully-correlated problem. Thus, although the optimized potential of Talman et al^{30,31} may be the exchange-only Kohn-Sham potential, our theory provides a more physically accurate representation of the potential throughout space in that both the ground-state energies as well as ionization potentials are determined accurately. In this context we note that if one were to calculate the expectation value of the Hamiltonian with respect to a Slater determinant whose orbitals are the solutions of the Kohn-Sham equations with the full exchange-correlation potential, the result¹⁰ for the total energy thus obtained would lie above those of exchange-only Kohn-Sham theory. The overall accuracy of the potential is also reflected by the fact that for the nonuniform electron gas at metal surfaces, the correct image

potential structure is obtained asymptotically. Additional calculations that could further substantiate the accuracy of the potential would be to compare in the exchange-only approximation the sum of the highest occupied orbital eigenenergies of atoms as they are ionized with the corresponding sum of the experimental ionization potentials. Again, since the exchange potential in our formalism is the exact exchange-correlation potential in the exterior regions of the atom where a major contribution to the highest occupied eigenvalues comes from, the sum of the highest occupied eigenvalues should approximate well the total experimental ground-state energies.

In Kohn-Sham density-functional theory,⁹ the kinetic energy is that of non-interacting electrons having the true density. For our exchange-correlation potential to be the same as the Kohn-Sham potential for the fully-correlated system requires the addition of a term which takes into consideration the difference between the kinetic energy of the interacting and non-interacting electrons. We expect the contribution of such a term to our potential to be small, and therefore any physically reasonable approximation to the Coulomb hole charge density would lead to an effective potential that is very close to the exact one.

As a consequence of the physical interpretation provided, the method for determining an accurate local many-body potential is now understood. The exchange part of this potential is explicitly known, and therefore so is the asymptotic structure for the fully-correlated electron gas. An important direction for future research is therefore

the study and development of the Coulomb hole charge distribution from which the local correlation potential could then be determined. For the light atoms, this could initially be done by the use of correlated or configuration-interaction type wavefunctions. For high density metals, the structure of the Fermi-Coulomb hole at surfaces could be determined within the random phase approximation.⁶⁵ With the knowledge of the Fermi-Coulomb hole, the position of the image plane can easily be determined. Furthermore, from the Fermi-Coulomb hole one can also obtain and study the structure of the Coulomb hole because the structure of the Fermi hole at metallic surfaces is known. The random phase approximation is also valid in the interior of the atom and consequently the Coulomb hole in atoms could also be studied in this manner.

Another area of important application of our formalism, which we have not focused upon in this thesis, is the study of excited states of many-electron systems. As noted, our formalism is not restricted by the variational principle for the energy to being only a ground-state theory. Thus the excited states of electronic systems can also be studied via this formalism. Since the Fermi-Coulomb hole charge distribution of electrons in the ground and excited states differ, the corresponding potentials will also be different. A problem of particular significance in this category is that of the fundamental gap^{64,66} in semiconductors and insulators. The fundamental gap is defined as the difference between the lowest conduction-band and the highest valence-band energies. In recent work⁶⁷ it has been shown that the exact Kohn-Sham band gap differs

from the true gap by a discontinuity in the functional derivative of the exchange-correlation energy functional. The advantage of studying the fundamental gap as an excited state problem via our formalism is that the question of the derivative discontinuity⁶⁷ is circumvented. Furthermore, with a knowledge of the band gap, estimates of the magnitude of this derivative discontinuity of Kohn-Sham theory could also be obtained.

Appendix A

**EXPRESSION FOR THE FERMI HOLE AND THE CORRESPONDING ELECTRIC FIELD
FOR CLOSED SUBSHELL ATOMS**

For closed subshell atoms, the electronic wavefunction at \mathbf{r} is given as

$$\Psi_{nlm}(\mathbf{r}) = R_{nl}(r) Y_{lm}(\theta, \varphi) , \quad (\text{A.1})$$

where $R_{nl}(r)$ is the radial part of the wavefunction, and $Y_{lm}(\theta, \varphi)$, the angular part is the spherical harmonic of order (l, m) . The expressions for the single-particle density matrix $\gamma(\mathbf{r}, \mathbf{r}')$ [Eq. 1.21] and the electronic density $\rho(\mathbf{r})$ [Eq. 1.9] for closed subshell atoms in terms of these wavefunctions can now be written as

$$\gamma(\mathbf{r}, \mathbf{r}') = \frac{1}{2\pi} \{ \sum_{nl} (2l+1) P_1(\cos\gamma) R_{nl}(r) R_{nl}(r') \} , \quad (\text{A.2})$$

where γ is the angle between \mathbf{r} and \mathbf{r}' , and

$$\rho(\mathbf{r}) = \frac{1}{2\pi} \sum_{nl} (2l+1) R_{nl}^2(r) . \quad (\text{A.3})$$

It is evident from the above expression, that the electronic density is spherically symmetric, as it must be. Substituting Eqs. (A.2) and (A.3) into the expression for the Fermi hole [Eq. 1.20], we obtain the exchange charge density at \mathbf{r}' for an electron at \mathbf{r} as

$$\rho_x(\mathbf{r}, \mathbf{r}') = \frac{\{ \sum_{nl} (2l+1) P_1(\cos\gamma) R_{nl}(r) R_{nl}(r') \}^2}{2\pi \{ \sum_{nl} (2l+1) R_{nl}^2(r) \}} . \quad (\text{A.4})$$

From the expression above we see that the Fermi hole charge density depends only on the angle γ between \mathbf{r} and \mathbf{r}' , and not on the azimuthal angle between them. As a consequence, the electric field due to the total charge of the Fermi hole is in the direction of \mathbf{r} , and a function of r only. Thus the electric field can be written as

$$\boldsymbol{\epsilon} = \hat{\mathbf{r}}\epsilon_r(r) , \quad (\text{A.5})$$

where $\hat{\mathbf{r}}$ is the unit vector, and $\epsilon_r(r)$ the component of the field in the \mathbf{r} direction. From Eq. (A.5) it is also clear that the curl $(\nabla \times \boldsymbol{\epsilon})$ of this field is zero. Substituting the expression for the Fermi hole from Eq. (A.4) into Eq. (2.2) for the electric field, $\epsilon_r(r)$ can be written as

$$\epsilon_r(r) = \frac{1}{4\pi\rho(r)} \int \frac{\{\sum_{nl} (2l+1)P_l(\cos\gamma)R_{nl}(r)R_{nl}(r')\}^2}{(r^2 + r'^2 - 2rr'\cos\gamma)^{3/2}} \cdot (r-r'\cos\gamma)r'^2 dr'd(\cos\gamma) . \quad (\text{A.6})$$

The $\cos\gamma$ integral in the expression above can be done analytically. The r' integral is performed numerically. With this electric field, the potential $W_{\mathbf{x}}$, which is the work done in moving the electron in the field, is given as

$$W_{\mathbf{x}}(r) = -\int_{\infty}^r \epsilon_r(r') dr' . \quad (\text{A.7})$$

We now take a specific example of the Ar atom and write the expression for the electric field. The electronic configuration of the Ar atom is $1s^2, 2s^2 2p^6, 3s^2 3p^6$. After doing the angular integration over $\cos\gamma$, the electric field is as follows:

$$\begin{aligned}
\epsilon_r(r) = & \frac{1}{4\pi\rho(r)} \int_0^r dr' \left[2 \frac{r'^2}{r^2} \{ \Sigma_n R_{ns}(r) R_{ns}(r') \}^2 + \right. \\
& + \left\{ \frac{36r'^4}{5r^4} + \frac{6r'^2}{r^2} \right\} \{ \Sigma_n R_{np}(r) R_{np}(r') \}^2 \\
& + \left. 8 \frac{r'^3}{r^3} \{ \Sigma_n R_{ns}(r) R_{ns}(r') \} \{ \Sigma_n R_{np}(r) R_{np}(r') \} \right] \\
& - \frac{1}{4\pi\rho(r)} \int_r^\infty dr' \left[\frac{24r}{5r'} \{ \Sigma_n R_{np}(r) R_{np}(r') \}^2 + \right. \\
& + \left. 4 \{ \Sigma_n R_{ns}(r) R_{ns}(r') \} \{ \Sigma_n R_{np}(r) R_{np}(r') \} \right] .(A.8)
\end{aligned}$$

Thus the field can now be obtained by performing the r' integrals in the above expression numerically. This expression is general in that it can also be used to calculate the electric field due to the Fermi hole for those atoms that have only the s and p shells filled.

Appendix B

FERMI HOLE AT METALLIC SURFACES

In this Appendix we derive Eq. (3.4) for the Fermi hole at metal surfaces. On substituting the expression for the wavefunction for electrons at metal surfaces [Eq. (3.1)] into the expression for the Fermi hole [Eq. (1.20)] we obtain

$$\rho_{\mathbf{x}}(\mathbf{r}, \mathbf{r}') \Big|_{\mathbf{x}_{\parallel}=0} = \frac{1}{[\rho(\mathbf{r})/2]} \left(\frac{2}{V} \right)^2 \sum_{\mathbf{k}, \mathbf{k}_{\parallel}} \sum_{\mathbf{k}', \mathbf{k}'_{\parallel}} \Theta(k_F^2 - k^2 - k_{\parallel}^2) \Theta(k_F^2 - k'^2 - k'_{\parallel}^2) \cdot e^{i(\mathbf{k}_{\parallel} - \mathbf{k}'_{\parallel}) \cdot \mathbf{x}_{\parallel}} \varphi_{\mathbf{k}}^*(\mathbf{x}) \varphi_{\mathbf{k}', \mathbf{k}'_{\parallel}}^*(\mathbf{x}') \varphi_{\mathbf{k}}(\mathbf{x}') \varphi_{\mathbf{k}, \mathbf{k}_{\parallel}}(\mathbf{x}) \quad (\text{B.1})$$

$$= \frac{1}{2\pi^6 \rho(\mathbf{r})} \int_0^{k_F} dk \int_0^{k_F} dk' \varphi_{\mathbf{k}}^*(\mathbf{x}) \varphi_{\mathbf{k}', \mathbf{k}'_{\parallel}}^*(\mathbf{x}') \varphi_{\mathbf{k}}(\mathbf{x}') \varphi_{\mathbf{k}, \mathbf{k}_{\parallel}}(\mathbf{x}) \cdot \left(\int_0^{(k_F^2 - k^2)^{1/2}} dk_{\parallel} \int_0^{2\pi} d\theta e^{ik_{\parallel} |\mathbf{x}_{\parallel}| \cos\theta} \right) \cdot$$

$$\left(\int_0^{(k_F^2 - k'^2)^{1/2}} dk'_{\parallel} \int_0^{2\pi} d\theta' e^{ik'_{\parallel} |\mathbf{x}_{\parallel}| \cos\theta'} \right) \cdot (\text{B.2})$$

Now the integral

$$\int_0^{(k_F^2 - k^2)^{1/2}} dk_{\parallel} \int_0^{2\pi} d\theta e^{ik_{\parallel} |\mathbf{x}_{\parallel}| \cos\theta} = 2\pi \int_0^{(k_F^2 - k^2)^{1/2}} dk_{\parallel} J_0(k_{\parallel} |\mathbf{x}_{\parallel}|) \\ = 2\pi \frac{(k_F^2 - k^2)^{1/2}}{|\mathbf{x}_{\parallel}|} J_1[(k_F^2 - k^2)^{1/2} |\mathbf{x}_{\parallel}|] \quad (\text{B.3})$$

so that Eq. (B.2) becomes

$$\rho_{\mathbf{x}}(\mathbf{r}, \mathbf{r}') = \frac{2}{\pi^4 \rho(\mathbf{r})} \left| \int_0^{k_F} dk \varphi_k^*(\mathbf{x}) \varphi_k(\mathbf{x}') \frac{(k_F^2 - k^2)^{1/2}}{x_{||}} J_1[(k_F^2 - k^2)^{1/2} x_{||}] \right|^2 \quad (\text{B.4})$$

Here $J_0(x)$ and $J_1(x)$ are the zeroth- and first-order Bessel functions, respectively. Changing to the dimensionless variables $q = k/k_F$, $y = k_F x$, $y'_{||} = k_F x_{||}$, and denoting $|y'_{||}|$ by R one gets the universal function

$$\frac{\rho_{\mathbf{x}}(y, y'; R)}{(\bar{\rho}/2)} = \frac{36}{\rho_n(y)} \left| \int_0^1 dq \varphi_q^*(y) \varphi_q(y') \frac{(1-q^2)^{1/2}}{y'_{||}} J_1[(1-q^2)^{1/2} R] \right|^2, \quad (\text{B.5})$$

which is Eq. (3.4). This is the average exchange charge density or Fermi hole at (y', R) for an electron at y .

Appendix C

**ASYMPTOTIC BEHAVIOR OF THE PLANAR-AVERAGED FERMI HOLE
AT METALLIC SURFACES**

The planar-averaged Fermi hole at a metal surface defined by Eq. (3.9) may be written³⁵ as

$$\frac{\rho_x(y, y')}{(3k_F/\pi)} = \frac{F(y, y')}{\rho_n(y)} \quad , \quad (C.1)$$

where

$$F(y, y') = 2 \int_0^1 dq (1-q^2) \int_0^q dq' [\varphi_{qq'}(y, y') + \varphi_{qq'}(y', y)] \quad , \quad (C.2)$$

and where

$$\varphi_{qq'}(y, y') = \varphi_q^*(y) \varphi_{q'}^*(y') \varphi_q(y') \varphi_{q'}(y) \quad . \quad (C.3)$$

In this Appendix we derive the y' dependence of the planar-averaged Fermi hole deep in the bulk (i.e. for $y' \ll 0$) independent of the position y of the electron. For real φ 's, Eq. (C.1) may be rewritten as

$$\rho_x(y, y') = \frac{36k_F}{\pi \rho_n(y)} \int_0^1 dq (1-q^2) \varphi_q(y') \varphi_q(y) \int_0^q dq' \varphi_{q'}(y') \varphi_{q'}(y) \quad . \quad (C.4)$$

For $y' \ll 0$, $\varphi_{q'}(y')$ can be approximated as $\sin(q'y')$ by ignoring the

phase shift $\delta(q')$ so that

$$\begin{aligned}
 \int_0^q dq' \phi_{q'}(y') \phi_{q'}(y) &= \int_0^q dq' \sin(q'y') \phi_{q'}(y) \\
 &= -\frac{\cos(qy')}{y'} \phi_q(y) + \frac{1}{y'^2} \sin(qy') \frac{d}{dq} \phi_q(y) - \\
 &\quad - \frac{1}{y'^2} \int_0^q dq' \sin(q'y') \frac{d^2 \phi_{q'}(y)}{dq'^2} \quad . \quad (C.4)
 \end{aligned}$$

Now for wavefunctions which are either exponential (as they are in the classically forbidden region) or oscillatory (as in the metal),

$$\frac{d^2 \phi_{q'}(y)}{dq'^2} \sim y^2 \phi_{q'}(y) \quad (C.5)$$

[In the case of the linear-potential model $d^2 \phi_{q'}(y)/dq'^2 \sim y \phi_{q'}(y)$].

Substituting Eq. (C.5) into Eq. (C.4) we obtain

$$\begin{aligned}
 \int_0^q dq' \phi_{q'}(y') \phi_{q'}(y) &= -\frac{\cos(qy')}{y'} \phi_q(y) + \frac{1}{y'^2} \sin(qy') \frac{d}{dq} \phi_q(y) - \\
 &\quad - \left(\frac{y}{y'}\right)^2 \int_0^q dq' \sin(q'y') \phi_{q'}(y) \quad . \quad (C.6)
 \end{aligned}$$

The last integral in Eq. (C.6) is the same as the one we started with, so that the last term is of $O(y'^{-3})$ and therefore may be neglected.

Thus we may write

$$\begin{aligned}
 \rho_x(y, y' \rightarrow -\infty) &\sim \frac{36k_F}{\pi\rho_n(y)} \int_0^1 dq(1-q^2) \sin(qy') \phi_q(y) \quad . \\
 &\quad \left(- \frac{\cos(qy')}{y'} \phi_q(y) + \frac{\sin(qy')}{y'^2} \frac{d}{dq} \phi_q(y) \right) \\
 &= \frac{1}{y'^2} \left(\frac{9k_F}{\pi\rho_n(y)} \int_0^1 dq(1-q^2) \frac{d}{dq} [\phi_q^2(y)] \right) - \\
 &\quad - \frac{1}{y'} \left(\frac{18k_F}{\pi\rho_n(y)} \int_0^1 dq(1-q^2) \sin(2qy) \phi_q^2(y) \right) - \\
 &\quad - \frac{1}{y'^2} \left(\frac{9k_F}{\pi\rho_n(y)} \int_0^1 dq(1-q^2) \cos(2qy') \frac{d}{dq} [\phi_q^2(y)] \right) \quad . \\
 &\hspace{20em} (C.7)
 \end{aligned}$$

The integrals in the second and the third terms are rapidly varying functions for $y' \rightarrow -\infty$, so that retaining the leading term of Eq. (C.7)

we have

$$\begin{aligned} \rho_x(y, y' \rightarrow -\infty) &\sim \frac{1}{y'^2} \left(\frac{9k_F}{\pi\rho_n(y)} \int_0^1 dq(1-q^2) \frac{d}{dq}[\varphi_q^2(y)] \right) \\ &= -\frac{1}{y'^2} \left(\frac{18k_F}{\pi\rho_n(y)} \int_0^1 dq(1-q^2) q\varphi_q^2(y) \right) \quad . \quad (C.8) \end{aligned}$$

Thus the leading term in $\rho_x(y, y')$ as $y' \rightarrow -\infty$ goes as $(y')^{-2}$.

Appendix D

EXACT SLATER POTENTIAL AT METALLIC SURFACES

In this Appendix we derive the expression for the exact Slater potential of Eq. (2.18) for electrons at metallic surfaces. Since the Fermi hole $\rho_{\mathbf{x}}(\mathbf{r}, \mathbf{r}')$ depends [see Eq. (B.4)] only on the electron position \mathbf{x} , the position of the plane in which the charge is being considered \mathbf{x}' , and the radial distance $|\mathbf{x}_{\parallel}|$ from the axis of electron removal, it has cylindrical symmetry about the axis of electron removal. The Slater potential can therefore be written as

$$v_{\mathbf{x}}^{\text{Sl}}(\mathbf{x}) = 2\pi \int_{-\infty}^{\infty} dx' \int_0^{\infty} d|\mathbf{x}_{\parallel}| \frac{|\mathbf{x}_{\parallel}| \rho_{\mathbf{x}}(\mathbf{x}, \mathbf{x}', |\mathbf{x}_{\parallel}|)}{[(x-x')^2 + |\mathbf{x}_{\parallel}|^2]^{1/2}} \quad (\text{D.1})$$

Now substituting for $\rho_{\mathbf{x}}(\mathbf{x}, \mathbf{x}', |\mathbf{x}_{\parallel}|)$ from Eq. (B.4) we get

$$v_{\mathbf{x}}^{\text{Sl}}(\mathbf{x}) = \frac{4}{\pi^3 \rho(\mathbf{x})} \int_{-\infty}^{\infty} dx' \int_0^{\infty} d|\mathbf{x}_{\parallel}| \frac{|\mathbf{x}_{\parallel}|}{[(x-x')^2 + |\mathbf{x}_{\parallel}|^2]^{1/2}} \left| \int_0^{k_F} dk \varphi_k^*(\mathbf{x}) \varphi_k(\mathbf{x}') \frac{(k_F^2 - k^2)^{1/2}}{|\mathbf{x}_{\parallel}|} J_1[(k_F^2 - k^2)^{1/2} |\mathbf{x}_{\parallel}|] \right|^2 \quad (\text{D.2})$$

Now changing to the dimensionless variables $y = k_F x$, $y' = k_F x'$, $R = k_F |\mathbf{x}_{\parallel}|$, $q = k/k_F$ and $\rho_n(y) = \rho(\mathbf{x})/\bar{\rho}$, where $\bar{\rho} = k_F^3/3\pi^2$, gives

$$V_{\mathbf{x}}^{\text{Sl}}(\mathbf{x}) = \frac{12k_{\text{F}}}{\pi\rho_{\text{n}}(\mathbf{y})} \int_{-\infty}^{\infty} d\mathbf{y}' \int_0^{\infty} dR \frac{R}{[(\mathbf{y}-\mathbf{y}')^2 + R^2]^{1/2}} \cdot$$

$$\left| \int_0^1 dq \varphi_q^*(\mathbf{y}) \varphi_q(\mathbf{y}') \frac{(1-q^2)^{1/2}}{R} J_1[(1-q^2)^{1/2}R] \right|^2 .$$

(D.3)

Now defining

$$g(\mathbf{y}, \mathbf{y}', R) = \left| \int_0^1 dq \varphi_q^*(\mathbf{y}) \varphi_q(\mathbf{y}') Q J_1[(1-q^2)^{1/2}R]/R \right|^2 , \quad (\text{D.4})$$

where $Q = (1-q^2)^{1/2}$, we can write the Slater potential in terms of a universal function as

$$\frac{V_{\mathbf{x}}^{\text{Sl}}(\mathbf{y})}{(3k_{\text{F}}/2\pi)} = \frac{8}{\rho_{\text{n}}(\mathbf{y})} \int_{-\infty}^{\infty} d\mathbf{y}' \int_0^{\infty} dR \frac{R g(\mathbf{y}, \mathbf{y}', R)}{[(\mathbf{y}-\mathbf{y}')^2 + R^2]^{1/2}} , \quad (\text{D.5})$$

which is Eq. (3.11).

Appendix E

**THE ELECTRIC FIELD ϵ_x AND THE POTENTIAL W_x DUE TO THE FERMI HOLE
AT METALLIC SURFACES**

In this Appendix we derive expressions for the electric field ϵ_x and the corresponding work done W_x due to the Fermi hole charge distribution at metallic surfaces. The Fermi hole at a jellium metal surface is symmetric about the axis of electron removal. Therefore, those components of the electric field which are parallel to the surface vanish. Thus the net field $\epsilon_x(x)$ is in the direction perpendicular to the surface and is given as

$$\epsilon_x(x) = -2\pi \int_{-\infty}^{\infty} dx' \int_0^{\infty} d|x_{\parallel}| \frac{|x_{\parallel}| |\rho_x(x, x', |x_{\parallel}|)}{[(x-x')^2 + |x_{\parallel}|^2]^{3/2}} (x-x') \quad , \quad (E.1)$$

which on changing to the dimensionless variables $y=k_F x$, $y'=k_F x'$, and $R=k_F |x_{\parallel}|$ becomes

$$\epsilon_x(y) = -2\pi \int_{-\infty}^{\infty} dy' \int_0^{\infty} dR \frac{R \rho_x(y, y', R)}{k_F [(y-y')^2 + R^2]^{3/2}} (y-y') \quad . \quad (E.2)$$

Now substituting for $\rho_x(y, y'; R)$ from Eq. (B.5) we have

$$\epsilon_x(y) = -\frac{12k_F^2}{\pi \rho_n(y)} \int_{-\infty}^{\infty} dy' \int_0^{\infty} dR \frac{R g(y, y', R)}{[(y-y')^2 + R^2]^{3/2}} (y-y') \quad . \quad (E.3)$$

which gives

$$\frac{\epsilon_x(y)}{(3k_F^2/2\pi)} = - \frac{8}{\rho_n(y)} \int_{-\infty}^{\infty} dy' \int_0^{\infty} dR \frac{Rq(y, y', R)}{[(y-y')^2 + R^2]^{3/2}} (y-y') \quad . \quad (E.4)$$

The potential $W_x(x)$ is the work done in bringing an electron from ∞ to its final position x and is therefore given as

$$W_x(x) = - \int_{-\infty}^x dx' \epsilon_x(x') \quad . \quad (E.5)$$

On substitution of Eq. (E.4) for the electric field into Eq. (E.5), we obtain universal function

$$\frac{W_x(y)}{(3k_F^2/2\pi)} = 8 \int_{-\infty}^y \frac{dy'}{\rho_n(y')} \int_{-\infty}^{\infty} dy'' \int_0^{\infty} dR \frac{Rq(y', y'', R)}{[(y'-y'')^2 + R^2]^{3/2}} (y'-y'') \quad . \quad (E.6)$$

REFERENCES

1. D.R. Hartree, The Calculation of Atomic Structures (John Wiley, New York 1957).
2. C.F. Fischer, The Hartree-Fock Method for Atoms (John Wiley, New York 1977).
3. J.C. Slater, Quantum Theory of Atomic Structure vol.II (McGraw Hill, New York 1960)
4. C.L. Pekeris, Phys. Rev. 112, 1649 (1958); *ibid* 115, 1216 (1959); *ibid* 126, 1470 (1962); *ibid* A4, 516 (1971).
5. V. Sahni and C.Q. Ma, Phys. Rev. 22, 5987 (1980); J.Bardeen, Phys. Rev. 49, 653(1936).
6. N.H. March in Theory of the Inhomogeneous Electron Gas, edited by S. Lundquist and N.H. March (Plenum, New York 1983).
7. P. Hohenberg and W. Kohn, Phys. Rev. 136, B864 (1964).
8. Atomic units are used ($e = m = h = 1$).
9. W. Kohn and L.J. Sham, Phys. Rev. 140, A1133 (1965).
10. V. Sahni and M. Levy, Phys. Rev. B33, 3869 (1986).
11. J. Harris and R.O. Jones, J. Phys. F4, 1170 (1974).
12. O. Gunnarsson and B.I. Lundquist, Phys. Rev. B13, 4274 (1976).
13. D.C. Langreth and J.P. Perdew, Solid State Commun. 17, 1425 (1975); B15, 2884 (1977).
14. V. Sahni, J. Gruenebaum and J.P. Perdew, Phys. Rev. B26, 4371 (1982).
15. W. Kohn and P. Vashishta in Ref. 6.
16. J.P. Perdew, R.G. Parr, M. Levy and J.L. Balduz, Phys. Rev. Lett. 49, 1691 (1982).
17. M. Levy, J.P. Perdew and V. Sahni, Phys. Rev. A30, 2745 (1984).
18. K. Schonhammer and O. Gunnarsson, Phys. Rev. B37, 3128 (1988).
19. D. Mearns, Phys. Rev. B38, 5906 (1988).
20. D. Mearns and W. Kohn, Phys. Rev. B39, 10669(1989).
21. M. Levy and J.P. Perdew, Phys. Rev. A32, 2010 (1985).

22. A. Williams and U. von Barth in Ref. 6.
23. D.C. Langreth and M.J. Mehl, Phys. Rev. Lett. 47, 446 (1981); Phys. Rev. B28, 1809 (1983).
24. J.P. Perdew, Phys. Rev. Lett. 55, 1665 (1985); J.P. Perdew and Y. Wang, Phys. Rev. B33, 8800 (1986).
25. J.P. Perdew, Phys. Rev. B33, 8822 (1986); erratum ibid 34, 7406 (1986).
26. R.O. Jones and O. Gunnarsson, Rev. Mod. Phys. 61, 689 (1989).
27. M.K. Harbola and V. Sahni, Phys. Rev. Lett. 62, 489 (1989).
28. J.C. Slater, Phys. Rev. 81, 385 (1951).
29. R.T. Sharp and G.K. Horton, Phys. Rev. 90, 3876 (1953).
30. J.D. Talman and W.F. Shadwick, Phys. Rev. A14, 36 (1976).
31. K. Aashamar, T.M. Luke and J.D. Talman, At. Data Nucl. Tables 22, 443 (1978).
32. J.C. Slater, T.M. Wilson and J.H. Wood, Phys. Rev. 179, 28 (1969).
33. N.D. Lang, Solid State Phys. 28, 225 (1973).
34. M.K. Harbola and V. Sahni, Phys. Rev. B37, 745 (1988).
35. V. Sahni and K.-P. Bohnen, Phys. Rev. B29, 1045 (1984); ibid B31, 7651 (1985).
36. M.K. Harbola and V. Sahni, Phys. Rev. B36, 5024 (1987).
37. V. Sahni, Surf. Sci. 213, 226 (1989).
38. M.K. Harbola and V. Sahni, Phys. Rev. B39, 10437 (1989).
39. Y. Li, M.K. Harbola, J.B. Krieger and V. Sahni, Phys. Rev. A40, (1989).
40. C.E. Moore, Ionization Potentials and Ionization Limits Derived from the Analysis of Optical Spectra, Nat. Stand. Ref. Data Ser., Nat. Bur. Stand. (U.S.) 34, (1970).
41. C.J. Nisteruk and H.J. Juretschke, J. Chem. Phys. 22, 2087 (1954).
42. M.K. Harbola and V. Sahni, Bull. Am. Phys. Soc. 33, 738 (1988).
43. V. Sahni, K.-P. Bohnen and M.K. Harbola, Phys. Rev. A37, 1895 (1988).

44. M.K. Harbola and V. Sahni (unpublished); L. Kleinman and V. Sahni in Density-Functional Theory of Many-Fermion Systems, Edited by S.B. Trickey (Advances in Quantum-Chemistry, Academic Press, 1989).
45. E. Clementi and C. Roetti, At. Data Nucl. Data Tables 14, 177 (1974).
46. C.-O. Almbladh and U. von Barth, Phys. Rev. B31, 3231 (1985).
47. L.J. Sham, Phys. Rev. B32, 3876 (1985).
48. D.M. Arnow, M.K. Harbola and V. Sahni, Bull. Am. Phys. Soc. 33, 277 (1988).
49. V. Sahni, C.Q. Ma and J.S. Flamholz, Phys. Rev. B18, 3931 (1978).
50. V. Sahni, J.B. Krieger and J. Gruenebaum, Phys. Rev. B15, 1941 (1977); V. Sahni and J. Gruenebaum, Solid State Commun. 21, 463 (1977).
51. N.D. Lang and W. Kohn, Phys. Rev. B1, 4555 (1970).
52. N.D. Lang and W. Kohn, Phys. Rev. B3, 1215 (1971).
53. M. Abramowitz and I.A. Stegun, Handbook of Mathematical Functions, (Dover, New York, 1965).
54. A. Sugiyama, J. Phys. Soc. Japan 15, 965 (1960).
55. D.C. Langreth, Phys. Rev. B5, 2842 (1972).
56. V. Sahni, J.B. Krieger and J. Gruenebaum, Phys. Rev. B12, 3503 (1975); V. Sahni and J. Gruenebaum, Phys. Rev. B15, 1929 (1977).
57. V. Sahni, J.P. Perdew and J. Gruenebaum, Phys. Rev. B23, 6512 (1981).
58. H.J. Juretschke, Phys. Rev. 92, 1140 (1953).
59. L. Miglio, M.P. Tosi and N.H. March, Surf. Sci. 111, 119 (1981).
60. N.D. Lang and W. Kohn, Phys. Rev. B7, 3541 (1973).
61. O. Gunnarsson, M. Jonson and B.I. Lundquist, Phys. Rev. B20, 3136 (1979).
62. J. Rudnick, Ph.D. thesis, University of California, San Diego, 1970 (unpublished).
63. T. Koopmans, Physica 1, 104 (1933).
64. J.P. Perdew and A. Zunger, Phys. Rev. B23, 5048 (1981).

65. J.E. Inglesfield and I.D. Moore, *Solid State Commun.* 26, 876 (1978).
66. S.G. Louie in Electronic Structure, Dynamics and Quantum Structural Properties of Condensed Matter, Edited by T.J. Deoreese and P.V. Camp. NATO ASI Series, Vol. 21 (Plenum, N.Y. 1984); R.A. Heaton, J.G. Harrison and C.C. Liu, *Phys. Rev.* B28, 5922 (1983); R.A. Heaton and C.C. Liu, *J. Phys. C* 17, 1853 (1984); W. Borman and P. Fulde, *Phys. Rev.* B35, 9569 (1987).
67. J.P. Perdew and M. Levy, *Phys. Rev. Lett.* 51, 1884 (1983); L.J. Sham and M. Schluter, *Phys. Rev. Lett.* 51, 1888 (1983).